11-11-2022

Caspase-8 inactivation drives autophagy-dependent inflammasome activation in myeloid cells.

Yung-Hsuan Wu

Shu-Ting Mo

I-Ting Chen

Fu-Yi Hsieh

Shie-Liang Hsieh

See next page for additional authors

Authors

Yung-Hsuan Wu, Shu-Ting Mo, I-Ting Chen, Fu-Yi Hsieh, Shie-Liang Hsieh, Jianke Zhang, and Ming-Zong Lai

IMMUNOLOGY

Caspase-8 inactivation drives autophagy-dependent inflammasome activation in myeloid cells

Yung-Hsuan Wu[1], Shu-Ting Mo[1], I-Ting Chen[1], Fu-Yi Hsieh[1], Shie-Liang Hsieh[2], Jinake Zhang[3], Ming-Zong Lai[1]*

Caspase-8 activity controls the switch from cell death to pyroptosis when apoptosis and necroptosis are blocked, yet how caspase-8 inactivation induces inflammasome assembly remains unclear. We show that caspase-8 inhibition via IETD treatment in Toll-like receptor (TLR)–primed *Fadd*$^{-/-}$*Ripk3*$^{-/-}$ myeloid cells promoted interleukin-1β (IL-1β) and IL-18 production through inflammasome activation. Caspase-8, caspase-1/11, and functional GSDMD, but not NLRP3 or RIPK1 activity, proved essential for IETD-triggered inflammasome activation. Autophagy became prominent in IETD-treated *Fadd*$^{-/-}$*Ripk3*$^{-/-}$ macrophages, and inhibiting it attenuated IETD-induced cell death and IL-1β/IL-18 production. In contrast, inhibiting GSDMD or autophagy did not prevent IETD-induced septic shock in *Fadd*$^{-/-}$*Ripk3*$^{-/-}$ mice, implying distinct death processes in other cell types. Cathepsin-B contributes to IETD-mediated inflammasome activation, as its inhibition or down-regulation limited IETD-elicited IL-1β production. Therefore, the autophagy and cathepsin-B axis represents one of the pathways leading to atypical inflammasome activation when apoptosis and necroptosis are suppressed and capase-8 is inhibited in myeloid cells.

INTRODUCTION

Caspase-8 was first identified as an initiator caspase of extrinsic apoptosis (*1*, *2*). Extracellular stimuli, such as FasL, induce caspase-8 activation through the binding of caspase-8 and adaptor FADD to death receptor (*3*). Active caspase-8 then induces activation of effector caspase-3, caspase-6, and caspase-7 for the execution of apoptosis. Caspase-8 also inhibits necroptosis by cleaving receptor-interacting protein kinase 1 (RIPK1) and possibly RIPK3. Deficiency in caspase-8, its adaptor FADD, or caspase-8 activity enables formation of the necroptosome complex containing RIPK1, RIPK3, and mixed lineage kinase domain-like (MLKL) upon stimulation by Toll-like receptors (TLRs) or tumor necrosis factor receptor (TNFR) (*4*–*6*). Recently, caspase-8 activity was shown to be a determinant in the switch to pyroptosis when apoptosis and necroptosis are inhibited (*7*, *8*). Expression of the protease-inactive form of caspase-8 triggered formation of apoptosis-associated speck-like protein containing a CARD (ASC) specks and subsequent caspase-1 activation.

Inflammasome assembly triggers proteolytic cleavage of procaspase-1 into active caspase-1, which converts the cytokine precursors pro–interleukin-1β (IL-1β) and pro–IL-18 into mature and biologically active IL-1β and IL-18 (*9*, *10*). Active caspase-1 also induces cleavage of gasdermin D (GSDMD) to execute pyroptosis (*11*–*13*). The NLR family pyrin domain containing 3 (NLRP3) inflammasome is the most well-characterized inflammasome type, and it is conventionally activated in two steps. The initial priming signal is triggered by pattern recognition receptors, which induces nuclear factor κβ (NF-κβ) activation and downstream transcription of pro–IL-1β and NLRP3. The subsequent activation signal provided by NLRP3 activators, such as pore-forming toxin or monosodium crystal, induces a conformational change in NLRP3 and consequent recruitment of ASC and caspase-1 to assemble the inflammasome complex. Caspase-8 is known to participate in inflammasome activation for IL-1β production in several different ways. Ligation of TLR3 and TLR4 promotes caspase-8–mediated processing of pro–IL-1β, which is independent of NLRP3 and caspase-1 (*14*). Dectin-1 engagement induces inflammasome activation, resulting in caspase-8–dependent generation of active IL-1β (*15*). Depletion of inhibitors of apoptosis protein (IAPs) by means of a second mitochondria-derived activator of caspases (SMAC) mimetic in TLR-primed myeloid cells was found to trigger caspase-8–mediated generation of IL-1β (*16*). Caspase-8 protease activity is essential in all of these inflammasome activation processes, since inhibiting caspase-8 activity suppresses the IL-1β generation in myeloid cells induced by TLR3, dectin-1, SMAC mimetic, or FasL (*14*–*16*).

Both FADD and caspase-8 are involved in mediating the priming and activation of canonical and atypical NLRP3 inflammasomes, as well as ASC oligomerization (*17*–*22*). Lipopolysaccharide (LPS)–induced expression of pro–IL-1β or NLRP3 was previously shown to be impeded in *Casp8*$^{-/-}$*Ripk3*$^{-/-}$ and *Fadd*$^{-/-}$*Ripk3*$^{-/-}$ macrophages (*18*, *21*). NLRP3 activator–induced inflammasome activation could be blocked by using a caspase-8 inhibitor in LPS-primed bone marrow–derived macrophages (BMDMs) (*18*). In contrast, caspase-8 deficiency in dendritic cells was observed to facilitate RIPK3-dependent LPS-induced assembly and the function of NLRP3 inflammasomes (*23*).

Autophagy is characterized by the cytosolic vacuole formed upon initiation of the vacuolar membrane, autophagosome formation, and lysosome clearance of engulfed proteins, among other processes (*24*). Excessive autophagosome formation leads to autophagic cell death, which is independent of other cell death processes, and it is suppressed by genetic inhibition of autophagy proteins (*25*). Autophagy can regulate apoptosis and necroptosis, representing a type of "autophagy-dependent cell death." Both caspase-8 and FADD mediate autophagic cell death and autophagy-dependent apoptosis. Knockdown of caspase-8 was shown to induce autophagic cell death in a human cell line (*26*). Moreover, down-regulation of FADD suppressed the cell death induced by the autophagy-associated protein Atg5 (*27*). Autophagy and cell death are promoted in activated

[1]Institute of Molecular Biology, Academia Sinica, Taipei 11529, Taiwan. [2]Genomic Research Center, Academia Sinica, Taipei 11529, Taiwan. [3]Department of Microbiology and Immunology, Kimmel Cancer Center, Thomas Jefferson University, Philadelphia, PA 19107, USA.
*Corresponding author. Email: mblai@gate.sinica.edu.tw

T cells in the absence of FADD or caspase-8 signaling (*28*), with the autophagosome membrane serving as a platform for caspase-8 and FADD to mediate apoptosis (*29*). Therefore, capase-8 and FADD participate in autophagy-associated cell death in a stimulus- and cell type–dependent manner.

In this study, we explored the biological processes involved in inflammasome activation upon capase-8 inactivation in myeloid cells when both apoptosis and necroptosis are suppressed. We used LPS-stimulated FADD and RIPK3 double-knockout myeloid cells (*30*) to demonstrate that inhibiting caspase-8 activity by means of IETD induced IL-1β and IL-18 production. Atypical inflammasome formation was characterized by ASC dimerization, and it was NLRP3 independent. In addition, autophagy/cathepsin-B preceded inflammasome formation and cell death, as autophagy/cathepsin-B inhibition attenuated IL-1β production and cell death in the *Fadd*$^{-/-}$*Ripk3*$^{-/-}$ myeloid cells. In contrast, IETD-induced septic shock in *Fadd*$^{-/-}$*Ripk3*$^{-/-}$ mice was independent of autophagy, cathepsin-B, caspase-1/11, and GSDMD, implying that distinct death processes operate in other cell types. Therefore, here, we identify autophagy/cathepsin-B as the cellular process specifically induced by inactivated caspase-8 that partly accounts for inflammasome activation and cell death in *Fadd*$^{-/-}$*Ripk3*$^{-/-}$ myeloid cells.

RESULTS

Caspase-8 inhibition elicits inflammasome activation in *Fadd*$^{-/-}$*Ripk3*$^{-/-}$ myeloid cells

To examine the process by which cell death switched to pyroptosis upon suppression of both apoptosis and necroptosis, we used RIPK3-deficient mice (fig. S1, A to C) to generate *Fadd*$^{-/-}$*Ripk3*$^{-/-}$ mice. Knockout of FADD and RIPK3 in the *Fadd*$^{-/-}$*Ripk3*$^{-/-}$ BMDMs was confirmed by immunoblots (Fig. 1A). Caspase-8 is known to mediate dectin-1–induced inflammasome activation (*15*). First, we examined how dectin-1–mediated inflammasome activation was affected in *Fadd*$^{-/-}$*Ripk3*$^{-/-}$ bone marrow–derived dendritic cells (BMDCs). Treatment with the dectin-1 agonists curdlan or Zymosan Depleted (Dzymosan, which lacks TLR-stimulating properties) induced similar levels of IL-1β production in *Fadd*$^{-/-}$*Ripk3*$^{-/-}$ relative to *Fadd*$^{+/-}$*Ripk3*$^{-/-}$ BMDCs (Fig. 1B). We then used z-IETD-fmk (IETD), a known inhibitor of caspase-8 processing (fig. S1D), to determine the effect of caspase-8 inactivation on this process. IL-1β production in *Fadd*$^{+/-}$*Ripk3*$^{-/-}$ BMDCs was suppressed by IETD (Fig. 1B), confirming the requirement for caspase-8 protease activity in inflammasome activation (*15*). In contrast, IL-1β generation in Dzymosan-treated *Fadd*$^{-/-}$*Ripk3*$^{-/-}$ cells was not affected by IETD, whereas it was greatly enhanced by IETD in curdlan-treated *Fadd*$^{-/-}$*Ripk3*$^{-/-}$ cells (Fig. 1B), suggesting that caspase-8 inactivation promotes inflammasome activation. Similarly, LPS alone did not induce IL-1β generation in *Fadd*$^{+/-}$*Ripk3*$^{-/-}$ or *Fadd*$^{-/-}$*Ripk3*$^{-/-}$ BMDCs, yet additional presence of IETD did stimulate IL-1β production in *Fadd*$^{-/-}$*Ripk3*$^{-/-}$ BMDCs (Fig. 1C). These results indicate that in the absence of FADD and RIPK3, inhibition of caspase-8 leads to TLR4- or dectin-1–mediated inflammasome activation in BMDCs.

We further examined the effect of IETD on cells stimulated with another TLR agonist, R848, and found that a combination of R848 and IETD also induced IL-1β production in *Fadd*$^{-/-}$*Ripk3*$^{-/-}$ cells (Fig. 1C). Similar to BMDCs, IETD cotreatment with LPS or R848 induced IL-1β production in *Fadd*$^{-/-}$*Ripk3*$^{-/-}$ BMDMs (Fig. 1D). Since pro–IL-18 is constitutively expressed in BMDMs, we examined whether TLR agonists could induce high-level IL-18 secretion in the presence of IETD in *Fadd*$^{-/-}$*Ripk3*$^{-/-}$ BMDMs and found that all TLR agonists we examined, including polyinosine-polycytidylic acid (poly(I:C)), did so (Fig. 1E). Both IL-1β and IL-18 were detected 6 to 8 hours after LPS + IETD treatment in *Fadd*$^{-/-}$*Ripk3*$^{-/-}$ BMDMs (fig. S1E). To exclude the possibility that the observed effect was due to incomplete inhibition of caspase-8, we applied IETD (10 μM) repeatedly (four times) and found that IL-1β production and cell viability of *Fadd*$^{-/-}$*Ripk3*$^{-/-}$ BMDMs and BMDCs were similar to values determined following single-dose IETD administration (10 μM) (fig. S2, A to D). Moreover, we increased the dose of IETD from 10 to 40 μM, and yet IL-1β production remained comparable in the *Fadd*$^{-/-}$*Ripk3*$^{-/-}$ BMDCs (fig. S2E). Application of the pan-caspase inhibitor QVD or zVAD at 40 μM induced very low IL-1β production (fig. S2E). These results illustrate that the amount of IETD we applied was not a limiting factor for the biological effects we observed. We also explored whether TLR signaling could be replaced by TNF stimulation but found that IETD and TNF cotreatment of *Fadd*$^{-/-}$*Ripk3*$^{-/-}$ BMDCs did not induce IL-1β production (Fig. 1F). Thus, the results of our IETD treatment experiments suggest a scenario in myeloid cells similar to previous reports demonstrating that caspase-8 inactivation promotes inflammasome activation upon blockade of apoptosis and necroptosis (*7*, *8*).

Reduced TLR signaling in *Fadd*$^{-/-}$*Ripk3*$^{-/-}$ myeloid cells

Our results show that impairment of caspase-8 protease activity elicits TLR- or dectin-1–mediated inflammasome activation in *Fadd*$^{-/-}$*Ripk3*$^{-/-}$ myeloid cells. Next, we examined the expression of inflammasome components during that process. Levels of procaspase-1, ASC, and pro–IL-18 were comparable between wild-type (WT; *Fadd*$^{+/+}$*Ripk3*$^{+/+}$), *Fadd*$^{+/-}$*Ripk3*$^{-/-}$, and *Fadd*$^{-/-}$*Ripk3*$^{-/-}$ BMDMs before and after IETD + LPS treatment (Fig. 2A). In contrast, expression levels of NLRP3 and pro–IL-1β were much lower in *Fadd*$^{-/-}$*Ripk3*$^{-/-}$ BMDMs than in WT or *Fadd*$^{+/-}$*Ripk3*$^{-/-}$ BMDMs after stimulation by IETD + LPS (Fig. 2A). Accordingly, induction of IL-1β by IETD + LPS in *Fadd*$^{-/-}$*Ripk3*$^{-/-}$ myeloid cells was not due to higher expression of pro–IL-1β relative to that in FADD-sufficient myeloid cells. We also detected a decreased level of TNF induced by LPS or poly(I:C), but not R848, in *Fadd*$^{-/-}$*Ripk3*$^{-/-}$ BMDMs with or without IETD (fig. S3A). A similar reduction in LPS-induced TNF was found in *Fadd*$^{-/-}$*Ripk3*$^{-/-}$ BMDCs relative to *Fadd*$^{+/-}$*Ripk3*$^{-/-}$ BMDCs (fig. S3B). This outcome contrasts with the normal TNF expression triggered by dectin-1 agonists in *Fadd*$^{-/-}$*Ripk3*$^{-/-}$ BMDCs (fig. S3C). The diminished induction of NLRP3, pro–IL-1β, and TNF was likely associated with attenuated TLR activation in *Fadd*$^{-/-}$*Ripk3*$^{-/-}$ BMDMs. LPS-induced NF-κB activation, marked by IKK [inhibitor of nuclear factor κB (IκB) kinase] phosphorylation and IκBα degradation, was attenuated in *Fadd*$^{-/-}$*Ripk3*$^{-/-}$ relative to *Fadd*$^{+/-}$*Ripk3*$^{-/-}$ BMDMs (Fig. 2B). A more profound reduction in LPS-stimulated mitogen-activated protein kinase (MAPK) signaling—as shown by decreased phosphorylation of c-Jun N-terminal kinase (JNK), p38, and extracellular signal–regulated kinase (ERK)—was observed in *Fadd*$^{-/-}$*Ripk3*$^{-/-}$ BMDMs (Fig. 2C). Thus, deficiency in both FADD and RIPK3 impairs LPS-induced activation of NF-κB and MAPK, consistent with previous studies reporting that FADD and RIPK3 are required for comprehensive innate signaling to prime inflammasome activation (*17*–*21*).

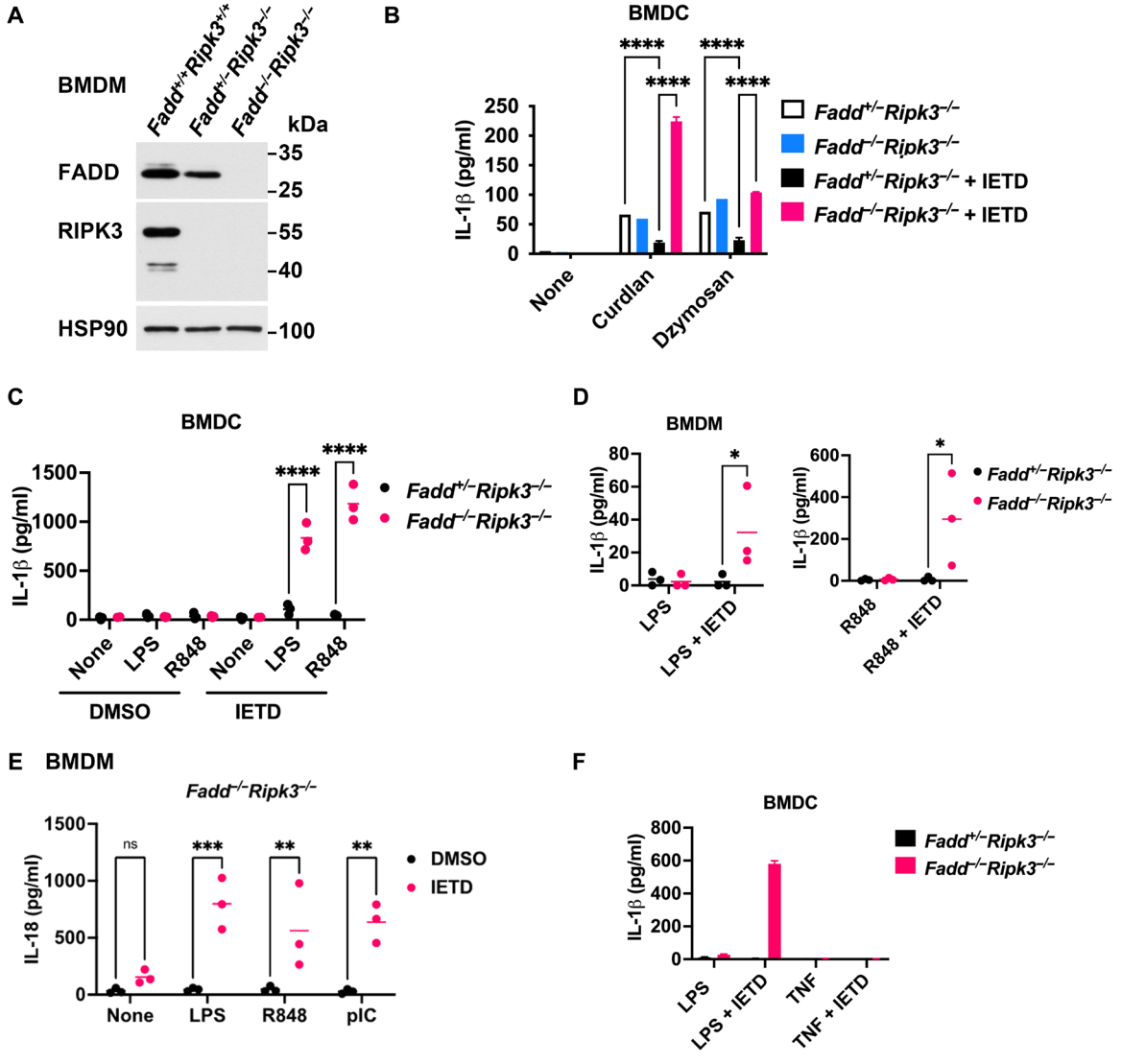

Fig. 1. Caspase-8 inhibition elicits TLR-mediated inflammasome activation in *Fadd*$^{-/-}$*Ripk3*$^{-/-}$ myeloid cells. (**A**) Expression of FADD and RIPK3 in *Fadd*$^{+/+}$*Ripk3*$^{+/+}$, *Fadd*$^{+/-}$*Ripk3*$^{-/-}$, and *Fadd*$^{-/-}$*Ripk3*$^{-/-}$ BMDMs, as determined by Western blot. (**B**) IETD induces IL-1β production in *Fadd*$^{-/-}$*Ripk3*$^{-/-}$ BMDCs stimulated with dectin-1 agonists. BMDCs were stimulated with curdlan (20 μg/ml) or Dzymosan (50 μg/ml), in the absence or presence of IETD (20 μM) for 8 hours, before analyzing IL-1β levels in culture supernatant by ELISA. Data are means ± SD of technical triplicates from one experiment and are representative of three independent experiments. (**C**) IETD + TLR agonists induce IL-1β production in *Fadd*$^{-/-}$*Ripk3*$^{-/-}$ BMDCs. BMDCs were stimulated with LPS (0.1 μg/ml) or R848 (1 μg/ml) in the presence or absence of IETD (20 μM) for 20 hours, and IL-1β levels were then determined. Data are means of three independent experiments. (**D** and **E**) IETD + TLR agonists induce IL-1β and IL-18 production in BMDMs. BMDMs were stimulated with LPS (0.1 μg/ml), R848 (1 μg/ml), or poly(I:C) (50 μg/ml) in the presence or absence of IETD (10 μM) for 20 hours, and then IL-1β (D) and IL-18 (E) production was determined. Data are means of three independent experiments. (**F**) IETD does not induce IL-1β production in TNF-stimulated *Fadd*$^{-/-}$*Ripk3*$^{-/-}$ BMDCs. BMDCs were stimulated with LPS (0.1 μg/ml) or TNF (50 ng/ml) in the presence or absence of IETD for 8 hours, and then IL-1β production was quantitated. **P* < 0.05, ***P* < 0.01, ****P* < 0.001, and *****P* < 0.0001 for two-way ANOVA followed by Si'ak's multiple comparisons test.

Recent studies suggested that inactive caspase-8 adopts a conformation distinct from active caspase-8, enabling the caspase-8 prodomain to nucleate ASC assembly for caspase-1 activation (*7*, *8*). We investigated whether IETD + R484 could induce ASC oligomerization in *Fadd*$^{-/-}$*Ripk3*$^{-/-}$ BMDCs, given that IETD + R484 treatment triggered a higher level of IL-1β production than observed for IETD + LPS treatment (Fig. 1C). First, R848 + nigericin treatment, which triggers canonical NLRP3 inflammasome formation, induced ASC dimer and oligomer formation in *Fadd*$^{+/-}$*Ripk3*$^{-/-}$ BMDCs (Fig. 2D), whereas weaker ASC dimer formation was detected in *Fadd*$^{-/-}$*Ripk3*$^{-/-}$ BMDCs subjected to the same treatment (Fig. 2D), likely attributable to the attenuated induction of NLRP3 by TLR (Fig. 2A). Consistent with that finding, the generation of p20 caspase-1 and p17 IL-1β was lower in *Fadd*$^{-/-}$*Ripk3*$^{-/-}$ BMDCs than in *Fadd*$^{+/-}$*Ripk3*$^{-/-}$ BMDCs when stimulated by LPS + nigericin (Fig. 2E, L + N). In contrast, no ASC dimer was detected in *Fadd*$^{+/-}$*Ripk3*$^{-/-}$ BMDCs stimulated by IETD + R484, whereas IETD + R484 induced dimerization of ASC in *Fadd*$^{-/-}$*Ripk3*$^{-/-}$ BMDCs (Fig. 2D).

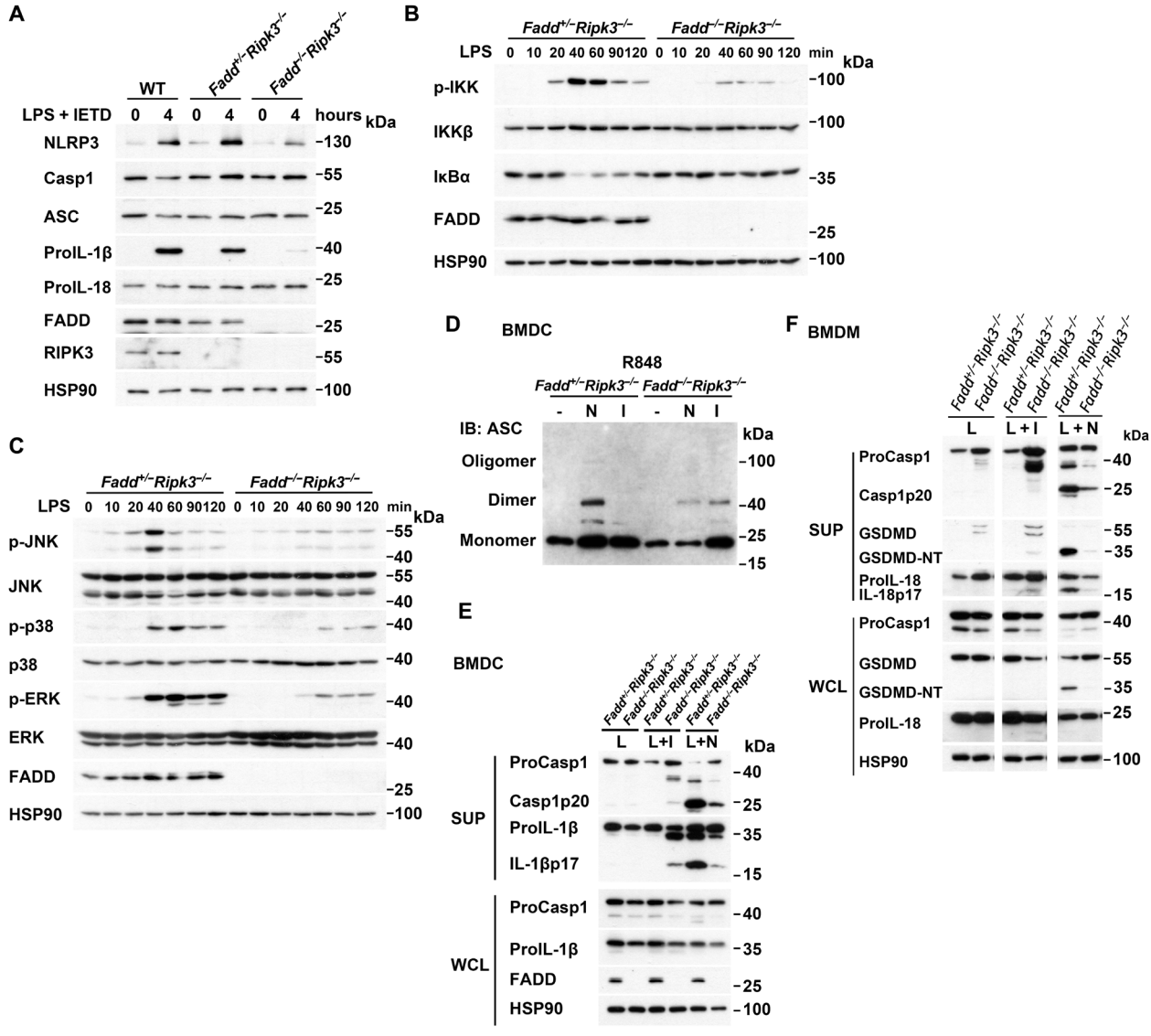

Fig. 2. Attenuated TLR signaling in *Fadd*$^{-/-}$*Ripk3*$^{-/-}$ myeloid cells. (**A**) *Fadd*$^{-/-}$*Ripk3*$^{-/-}$ BMDMs were stimulated with LPS (0.1 μg/ml) plus IETD (10 μM) for 4 hours, and levels of NLRP3, procaspase-1, ASC, and pro–IL-1β in cell lysates were then determined by immunoblotting. (**B** and **C**) Attenuated TLR activation signals in *Fadd*$^{-/-}$*Ripk3*$^{-/-}$ BMDMs. *Fadd*$^{-/-}$*Ripk3*$^{-/-}$ BMDMs were stimulated with LPS (0.1 μg/ml) for the indicated time frames. Cell lysates were then analyzed for p-IKK, IKKβ, and IκBα (B) and p-JNK, JNK, p-p38, p38, p-ERK, and ERK (C). (**D**) Formation of ASC pyroptosomes. BMDMs were stimulated with R848 (1 μg/ml) plus nigericin (N; 15 μM) or R848 (1 μg/ml) plus IETD (I; 10 μM). Total cell lysates were cross-linked by dextran sulfate sodium (DSS) and immunoblotted with anti-ASC. (**E**) BMDCs were stimulated with LPS (0.1 μg/ml) plus IETD (10 μM) for 6 hours (L + I) or LPS for 2 hours followed by nigericin (15 μM) for 20 min (L + N). Culture supernatants (SUP) were precipitated, and whole-cell lysates (WCL) were collected and analyzed for cleavage of procaspase-1 and pro–IL-1β. (**F**) BMDMs were stimulated with LPS (0.1 μg/ml) plus IETD (10 μM) for 10 hours (L + I) or LPS for 2 hours followed by nigericin (15 μM) for 20 min (L + N). Culture supernatants (SUP) were precipitated, and whole-cell lysates (WCL) were collected and analyzed for cleavage of procaspase-1, pro–IL-18, and GSDMD. Results are representative of two (B to D) or three (A, E, and F) independent experiments.

The formation of ASC specks is in agreement with the appearance of p20 caspase-1 and p17 IL-1β in *Fadd*$^{-/-}$*Ripk3*$^{-/-}$ BMDCs, but not in *Fadd*$^{+/-}$*Ripk3*$^{-/-}$ BMDCs treated with LPS + IETD (Fig. 2E, L + I). We found that production of IL-1β was lower in *Fadd*$^{-/-}$*Ripk3*$^{-/-}$ BMDMs than in *Fadd*$^{-/-}$*Ripk3*$^{-/-}$ BMDCs, but activation of caspase-1 and cleavage of pro–IL-18 were also apparent in *Fadd*$^{-/-}$*Ripk3*$^{-/-}$ BMDMs (Fig. 2F, L + I). Therefore, IETD plus a TLR agonist can trigger assembly of ASC into inflammasomes in *Fadd*$^{-/-}$*Ripk3*$^{-/-}$ myeloid cells, leading to the processing of procaspase-1 and generation of mature IL-1β/IL-18.

Requirement of caspase-8 and caspase-1/11 for IETD-induced inflammasome activation in *Fadd*$^{-/-}$*Ripk3*$^{-/-}$ cells

We found that inclusion of the pan-caspase inhibitor z-VAD-fmk with LPS, R848, or pIC induced very low levels of IL-1β or IL-18 production in *Fadd*$^{-/-}$*Ripk3*$^{-/-}$ BMDMs and BMDCs (fig. S2E and Fig. 3A), implying a requirement for other caspase(s) in atypical generation of those interleukins. Next, we delineated the requirement for caspase-8 in LPS/R848 + IETD–induced IL-1β production. Unlike for caspase-8 inactivation, knockdown of caspase-8 failed to trigger IL-1β secretion in LPS-treated *Fadd*$^{-/-}$*Ripk3*$^{-/-}$ or

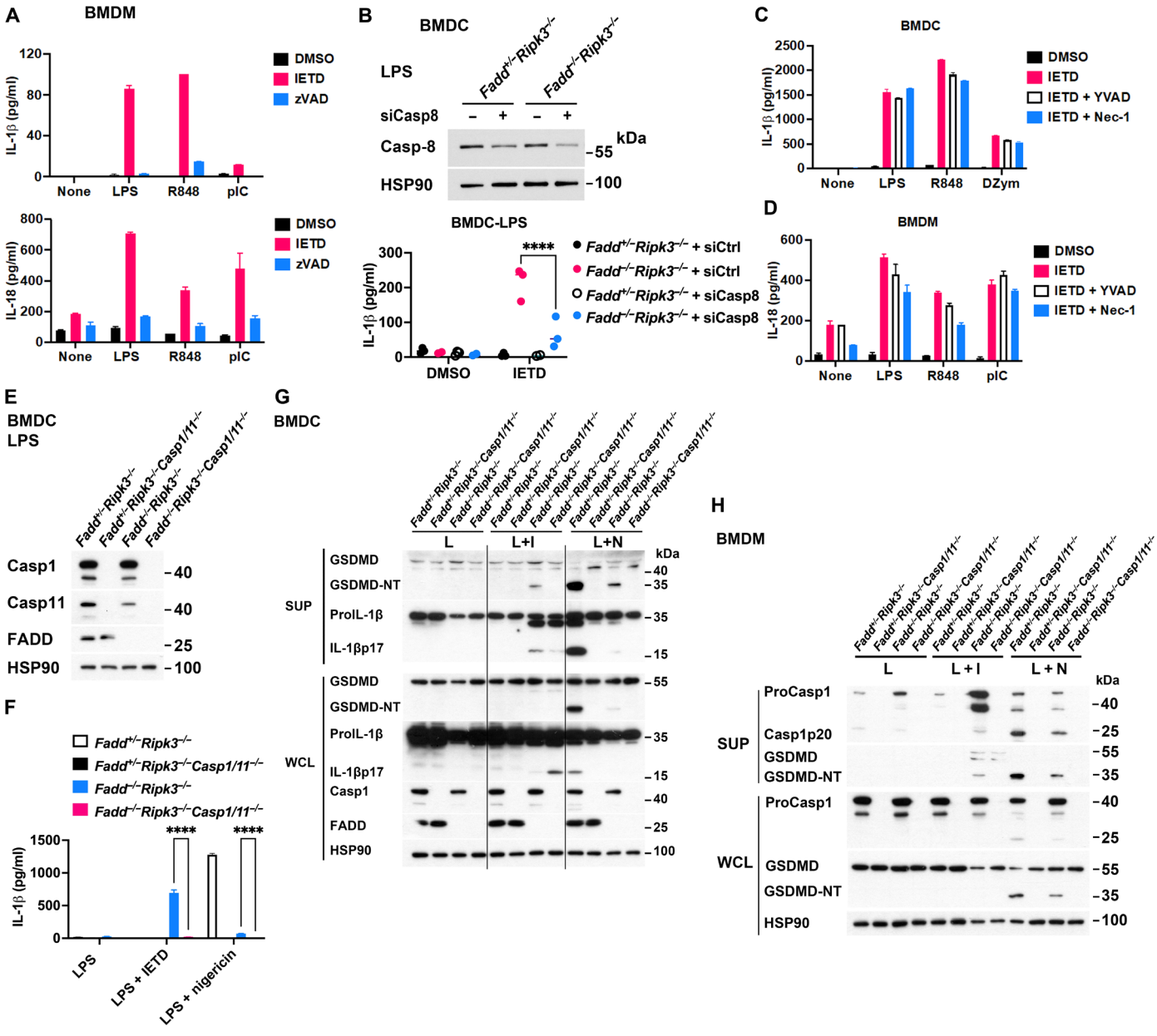

Fig. 3. Caspase-8 and caspase-1/11 are required for IETD-induced IL-1β/IL-18 production in *Fadd*$^{-/-}$*Ripk3*$^{-/-}$ myeloid cells. (**A**) BMDMs were stimulated with LPS (0.1 μg/ml), R848 (1 μg/ml), or poly(I:C) (50 μg/ml), without or with IETD (10 μM) or zVAD (40 μM) for 18 hours, before quantitating IL-1β. (**B**) BMDCs were transfected with control or caspase-8 siRNA for 24 hours. Caspase-8 was assessed by immunoblotting (upper panel). BMDCs were then treated with LPS plus IETD for 8 hours, before determining IL-1β production (lower panel). Data are means ± SD of three independent experiments. (**C** and **D**) BMDCs (C) or BMDMs (D) were stimulated with LPS, R848, Dzymosan (50 μg/ml), poly(I:C), IETD, YVAD (20 μM), or Nec-1 (40 μM), as indicated, for 8 hours (C) or 18 hours (D), before analyzing production of IL-1β (C) and IL-18 (D). (**E**) Levels of caspase-1, caspase-11, and FADD in BMDCs of indicated *casp1/11* genotypes. (**F**) IL-1β production by BMDCs of indicated genotypes treated with LPS plus IETD or LPS followed by nigericin. (**G** and **H**) BMDCs (G) and BMDMs (H) were treated with LPS plus IETD (L + I) for 6 hours (G) or 10 hours (H) or LPS for 2 hours followed by nigericin (15 μM) for 20 min (L + N). Culture supernatants and whole-cell lysates were analyzed for specific protein cleavage. Results (G and H) are representative of three independent experiments. Data are means ± SD of technical triplicates from one experiment and are representative of three independent experiments (A, C, D, and F). ****$P < 0.0001$ for two-way ANOVA followed by Sidak's multiple comparisons test (B and F).

Fadd$^{+/-}$*Ripk3*$^{-/-}$ BMDCs (Fig. 3B). Instead, knockdown of caspase-8 specifically inhibited LPS + IETD–induced IL-1β production in *Fadd*$^{-/-}$*Ripk3*$^{-/-}$ BMDCs (Fig. 3B), further evidencing the essentiality of caspase-8 in inflammasome activation. Therefore, specific inactivation of caspase-8 activity, while ensuring the respective protein remains intact, is responsible for IL-1β production in *Fadd*$^{-/-}$*Ripk3*$^{-/-}$ myeloid cells. We also determined whether IL-1β could be induced in the presence of RIPK3 by using *Fadd*$^{-/-}$*FADD:GFP*^{f}LyzM-Cre BMDMs (fig. S4A) and found that LPS alone induced IL-1β production in RIPK3-sufficient and FADD-deficient BMDMs, but it was completely blocked upon IETD treatment (fig. S4B), further supporting a requirement for caspase-8 activity. These results suggest

that in the absence of FADD, TLR signaling alone can induce caspase-8– and RIPK3-dependent inflammasome activation. However, in the absence of both FADD and RIPK3, specific inhibition of caspase-8 activity can still ensure inflammasome activation in the presence of TLR priming signaling.

Another irregularity we observed in our *Fadd*$^{-/-}$*Ripk3*$^{-/-}$ BMDMs was a reduction in RIPK1 protein expression (fig. S5A), despite *Ripk1* mRNA levels being comparable between *Fadd*$^{+/-}$*Ripk3*$^{-/-}$ and *Fadd*$^{-/-}$*Ripk3*$^{-/-}$ BMDMs (fig. S5B). We examined whether the protease inhibitor MG132, the lysosome fusion inhibitors chloroquine and ammonium chloride, or the RIPK1 kinase inhibitor necrostatin-1 (Nec-1) could restore protein levels of RIPK1 in *Fadd*$^{-/-}$*Ripk3*$^{-/-}$ BMDMs. However, with the exception of Nec-1, none of those inhibitors rescued RIPK1 expression levels in *Fadd*$^{-/-}$*Ripk3*$^{-/-}$ BMDMs (fig. S5C), implying that RIPK1 down-regulation is dependent on RIPK1 kinase activity.

Moreover, we used the caspase-1 inhibitor YVAD and Nec-1 to determine whether caspase-1 or RIPK1 activity is required for TLR/dectin-1 + IETD–induced IL-1β production in *Fadd*$^{-/-}$*Ripk3*$^{-/-}$ myeloid cells. Neither YVAD nor Nec-1 effectively interfered with the IL-1β and IL-18 production induced by TLR/dectin-1 + IETD in *Fadd*$^{-/-}$*Ripk3*$^{-/-}$ myeloid cells (Fig. 3, C and D). YVAD treatment, the efficacy of which was verified by almost complete suppression of canonical inflammasome-mediated generation of p20 caspase-1 and p17 IL-1β in BMDCs (fig. S6, L + N), was unable to inhibit LPS + IETD–induced processing of caspase-1 and IL-1β in *Fadd*$^{-/-}$*Ripk3*$^{-/-}$ BMDCs (fig. S6, L + I). These results indicate that caspase-1 and RIPK1 activity is not essential for IETD + LPS–triggered atypical inflammasome formation in *Fadd*$^{-/-}$*Ripk3*$^{-/-}$ myeloid cells. We further introduced *casp1/11*$^{-/-}$ into the respective myeloid cells (Fig. 3E). Knockout of caspase-1/11 eliminated IL-1β generation induced by LPS + nigericin in *Fadd*$^{+/-}$*Ripk3*$^{-/-}$ and *Fadd*$^{-/-}$*Ripk3*$^{-/-}$ BMDCs, as revealed by both enzyme-linked immunosorbent assay (ELISA) and immunoblots (Fig. 3, F and G, L + N). Caspase-1/11 deficiency abrogated IL-1β secretion triggered by LPS + IETD in *Fadd*$^{-/-}$*Ripk3*$^{-/-}$ BMDCs (Fig. 3, F and G, L + I). Therefore, the presence of caspase-1/11 is required for the generation of p17 IL-1β in *Fadd*$^{-/-}$*Ripk3*$^{-/-}$ myeloid cells.

Involvement of GSDMD in IETD-induced IL-1β secretion in *Fadd*$^{-/-}$*Ripk3*$^{-/-}$ myeloid cells

Inflammasome activation leads to active caspase-1 being generated, which in turns cleaves GSDMD, enabling oligomerization of the N-terminal part of GSDMD (GSDMD-NT) to form pores in cell membrane. GSDMD-mediated pore formation leads to cell lysis and pyroptotic death (*12*, *13*). GSDMD pores also facilitate transportation of active IL-1β and IL-18 across intact membrane and their release from live cells (*12*, *31*). In contrast to the prominent GSDMD cleavage induced by canonical inflammasomes detected in both cell lysates and culture supernatants, processing of GSDMD-NT could be detected mainly in supernatants from *Fadd*$^{-/-}$*Ripk3*$^{-/-}$ BMDCs (Figs. 2F, 3, G and H, and 4A). The generation of GSDMD-NT was blocked in *Casp1/11*$^{-/-}$ BMDCs and BMDMs (Fig. 3, G and H), suggesting that caspase-1/11 operates upstream of GSDMD cleavage. To further investigate whether the lack of active IL-1β secretion in *Fadd*$^{-/-}$*Ripk3*$^{-/-}$*Casp1/11*$^{-/-}$ myeloid cells was associated with the lack of N-GSDMD pore formation, we examined the impact of GSDMD by using disulfiram, which specifically inhibits GSDMD pore formation (*32*). Disulfiram at a concentration that does not trigger cell death (2.5 μM) attenuated the generation of IL-1β and IL-18 induced by LPS + IETD in *Fadd*$^{-/-}$*Ripk3*$^{-/-}$ myeloid cells (Fig. 4, B and C). We further generated control and *Fadd*$^{-/-}$*Ripk3*$^{-/-}$ mice with additional knockout of GSDMD (Fig. 4D). GSDMD knockout suppressed IETD-triggered IL-1β production in *Fadd*$^{-/-}$*Ripk3*$^{-/-}$ BMDCs (Fig. 4E). As a control, GSDMD deficiency impaired the IL-1β secretion induced by a canonical inflammasome-activating treatment (LPS + nigericin) in *Fadd*$^{+/-}$*Ripk3*$^{+/+}$ and *Fadd*$^{-/-}$*Ripk3*$^{-/-}$ BMDCs (Fig. 4F). These results provide evidence that GSDMD is involved in the release of IL-1β and IL-18 that is induced upon caspase-8 inactivation and is activated by caspase-1/11 cleavage in *Fadd*$^{-/-}$*Ripk3*$^{-/-}$ myeloid cells.

Caspase-8 has been reported to regulate NLRP3-dependent and NLRP3-independent inflammasome activation. We also determined the role of NLRP3 in LPS-induced caspase-8–mediated inflammasome activation in *Fadd*$^{-/-}$*Ripk3*$^{-/-}$ cells. NLRP3 knockout blocked the IL-1β secretion induced by canonical NLRP3 inflammasome activator LPS + nigericin in *Fadd*$^{-/-}$*Ripk3*$^{-/-}$ BMDMs and BMDCs (fig. S7A). However, NLRP3 deficiency did not prevent production of IL-1β and IL-18 in LPS + IETD–treated *Fadd*$^{-/-}$*Ripk3*$^{-/-}$ BMDMs (fig. S7B) or BMDCs (fig. S7C). Moreover, NLRP3 knockout did not affect levels of IL-1β and IL-18 in *Fadd*$^{-/-}$*Ripk3*$^{-/-}$ myeloid cells stimulated with R848 + IETD or CpG + IETD (fig. S7, B and C). Therefore, NLRP3 is dispensable for IETD-induced TLR-dependent atypical inflammasome activation.

IETD induces cell death in *Fadd*$^{-/-}$*Ripk3*$^{-/-}$ myeloid cells

As expected from FADD and RIPK3 deficiency, *Fadd*$^{-/-}$*Ripk3*$^{-/-}$ cells were fully resistant to apoptotic and necroptotic death (fig. S8, A and B). We found that LPS/pIC + IETD treatment elicited profound cell death in *Fadd*$^{-/-}$*Ripk3*$^{-/-}$ myeloid cells (Fig. 5A and fig. S8C), a phenomenon not recapitulated by LPS + zVAD (Fig. 5B). *Fadd*$^{-/-}$*Ripk3*$^{-/-}$ BMDCs were also susceptible to cell death induced by R848/Dzymosan + IETD treatments (fig. S8D). The vulnerability to LPS + IETD stimulation was observed mainly in myeloid cells, as *Fadd*$^{-/-}$*Ripk3*$^{-/-}$ mouse embryonic fibroblasts were fully resistant to the same treatment (fig. S8E). We detected multiple vesicular structures inside abundant dying *Fadd*$^{-/-}$*Ripk3*$^{-/-}$ BMDMs treated with LPS + IETD (Fig. 5C), as revealed by propidium iodide (PI) staining (*33*) (Fig. 5D).

We further elucidated the components required for IETD-induced cell death in *Fadd*$^{-/-}$*Ripk3*$^{-/-}$ myeloid cells. Caspase-8 knockdown restored the viability of IETD-treated *Fadd*$^{-/-}$*Ripk3*$^{-/-}$ myeloid cells (Fig. 5E), indicating that the physical presence of caspase-8 is indispensable. Just as GSDMD-knockout suppressed IL-1β generation in *Fadd*$^{-/-}$*Ripk3*$^{-/-}$ BMDMs and BMDCs (Fig. 4, A and B), GSDMD deficiency also abrogated cell death triggered by either canonical inflammasome activation or LPS + IETD (Fig. 5, F and G). In contrast, neither YVAD nor Nec-1 prevented IETD-triggered death in *Fadd*$^{-/-}$*Ripk3*$^{-/-}$ myeloid cells (Fig. 5H). Deficiency in both caspase-1 and caspase-11 also suppressed IETD-mediated death in *Fadd*$^{-/-}$*Ripk3*$^{-/-}$ BMDCs (Fig. 5I). Thus, similar involvement of intact caspase-8, caspase-1/11, and GSDMD in the generation of IL-1β/IL-18 and cell death in *Fadd*$^{-/-}$*Ripk3*$^{-/-}$ myeloid cells implies that the cell death is a consequence of atypical inflammasome activation.

IETD-induced septic shock in *Fadd*$^{-/-}$*Ripk3*$^{-/-}$ mice

We also determined the systemic impact of IETD-induced cell death. Intraperitoneal administration of IETD did not affect survival of control *Fadd*$^{+/-}$*Ripk3*$^{-/-}$ mice, but it was extensively fatal in

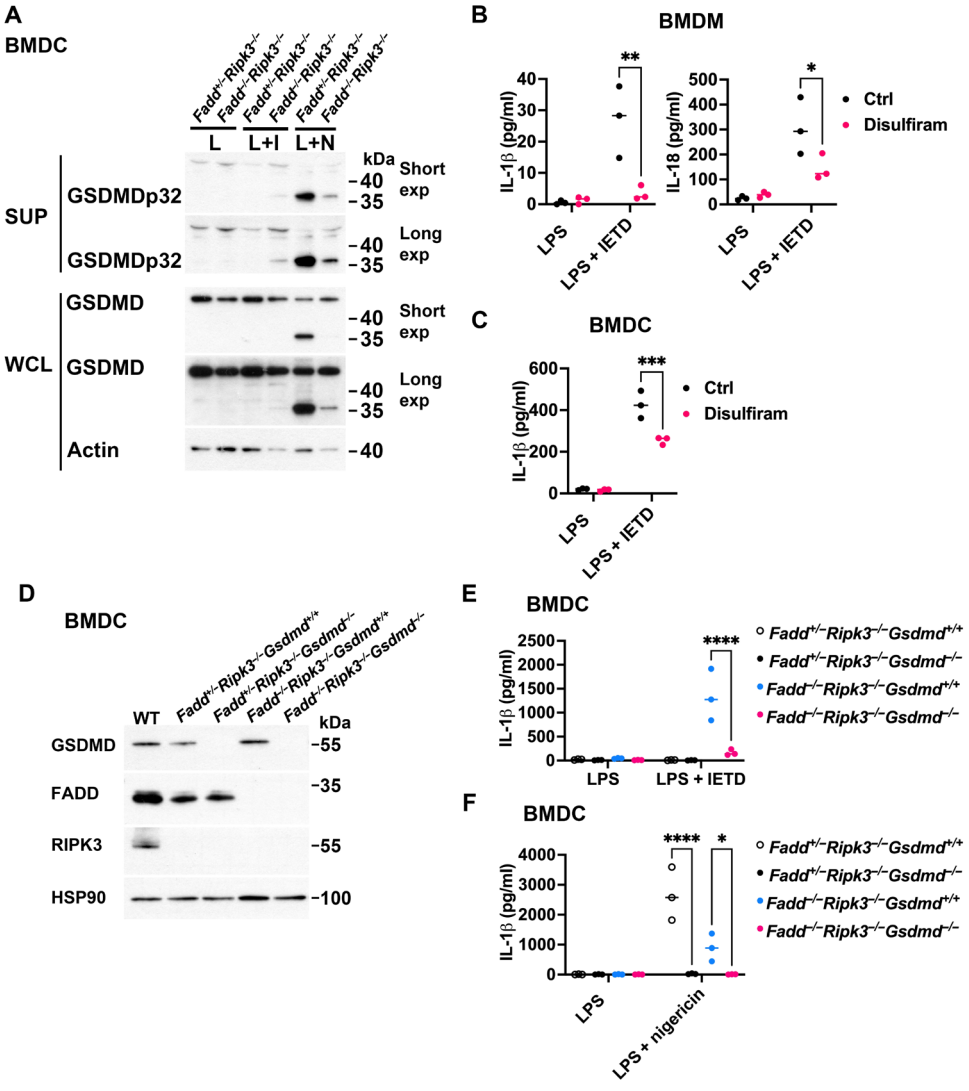

Fig. 4. Involvement of GSDMD in IL-1β/IL-18 production in IETD-treated *Fadd*$^{-/-}$*Ripk3*$^{-/-}$ myeloid cells. (**A**) BMDCs were treated with LPS plus IETD for 6 hours (L + I) or LPS for 2 hours followed by nigericin for 20 min (L + N). Culture supernatants and whole-cell lysates were collected and analyzed for cleavage of GSDMD. Short exp, 1-min exposure; Long exp, 3-min exposure. (**B** and **C**) *Fadd*$^{-/-}$*Ripk3*$^{-/-}$ BMDMs (B) and BMDCs (C) were treated with LPS (0.1 μg/ml) + IETD (10 μM) in the absence or presence of disulfiram (2.5 μM) for 16 hours before determining IL-1β (B and C) and IL-18 (B) production. (**D**) GSDMD, RIPK3, and FADD contents in *Fadd*$^{+/-}$*Ripk3*$^{+/+}$*Gsdmd*$^{+/-}$, *Fadd*$^{-/-}$*Ripk3*$^{-/-}$ *Gsdmd*$^{-/-}$, *Fadd*$^{-/-}$*Ripk3*$^{-/-}$*Gsdmd*$^{+/+}$, and *Fadd*$^{-/-}$*Ripk3*$^{-/-}$*Gsdmd*$^{-/-}$ BMDCs. (**E**) IL-1β production by *Fadd*$^{+/-}$*Ripk3*$^{+/+}$*Gsdmd*$^{+/-}$, *Fadd*$^{-/-}$*Ripk3*$^{-/-}$*Gsdmd*$^{-/-}$, *Fadd*$^{-/-}$*Ripk3*$^{-/-}$*Gsdmd*$^{+/+}$, and *Fadd*$^{-/-}$*Ripk3*$^{-/-}$*Gsdmd*$^{-/-}$ BMDCs treated with LPS + IETD for 16 hours. (**F**) IL-1β production by *Fadd*$^{+/-}$*Ripk3*$^{+/+}$*Gsdmd*$^{+/-}$, *Fadd*$^{-/-}$*Ripk3*$^{-/-}$*Gsdmd*$^{-/-}$, *Fadd*$^{-/-}$*Ripk3*$^{-/-}$*Gsdmd*$^{+/+}$, and *Fadd*$^{-/-}$*Ripk3*$^{-/-}$*Gsdmd*$^{-/-}$ BMDCs treated with LPS (0.1 μg/ml) for 3 hours followed by nigericin (20 μM) for 1 hour. Data (B, C, E, and F) are means of three independent experiments. *$P < 0.05$, **$P < 0.01$, ***$P < 0.001$, and ****$P < 0.0001$ for two-way ANOVA followed by Sidak's multiple comparisons test.

Fadd$^{-/-}$*Ripk3*$^{-/-}$ mice (Fig. 6A). We also observed elevated serum levels of IL-6 in *Fadd*$^{-/-}$*Ripk3*$^{-/-}$ mice 3 hours after IETD administration (Fig. 6B). We conducted peritoneal lavage of the mice to assess cell viability and cytokine levels. *Fadd*$^{-/-}$*Ripk3*$^{-/-}$ mice treated with IETD exhibited reduced peritoneal cell viability relative to control mice (Fig. 6C), as well as elevated expression of IL-1β and IL-6 (Fig. 6D). We also determined whether NLRP3 is required for IETD-induced septic shock in *Fadd*$^{-/-}$*Ripk3*$^{-/-}$ mice. NLRP3 knockout did not rescue *Fadd*$^{-/-}$*Ripk3*$^{-/-}$ mice from IETD-induced mortality (Fig. 6E). Consistent with this sensitivity to IETD, levels of IL-6 were higher in peritoneal cells isolated from IETD-primed *Fadd*$^{-/-}$*Ripk3*$^{-/-}$*Nlrp3*$^{-/-}$ mice compared to IETD-primed *Fadd*$^{-/-}$*Ripk3*$^{-/-}$*Nlrp3*$^{+/+}$ mice (Fig. 6F). Similar to IETD-induced inflammasome activation in *Fadd*$^{-/-}$*Ripk3*$^{-/-}$ myeloid cells, IETD induced septic shock in *Fadd*$^{-/-}$*Ripk3*$^{-/-}$ mice independently of NLRP3. Emricasan, a caspase inhibitor that also suppresses caspase-8, displayed a similar effect as IETD in terms of inducing septic shock in *Fadd*$^{-/-}$*Ripk3*$^{-/-}$ mice (Fig. 6G).

Autophagy mediates IETD-induced inflammasome activation in *Fadd*$^{-/-}$*Ripk3*$^{-/-}$ myeloid cells

We had observed that LPS + IETD treatment induced the appearance of small spherical vesicles in the cytosol of *Fadd*$^{-/-}$*Ripk3*$^{-/-}$ BMDMs (Fig. 5C), so we investigated the possibility that autophagy had been triggered. We found that the autophagy-specific inhibitor

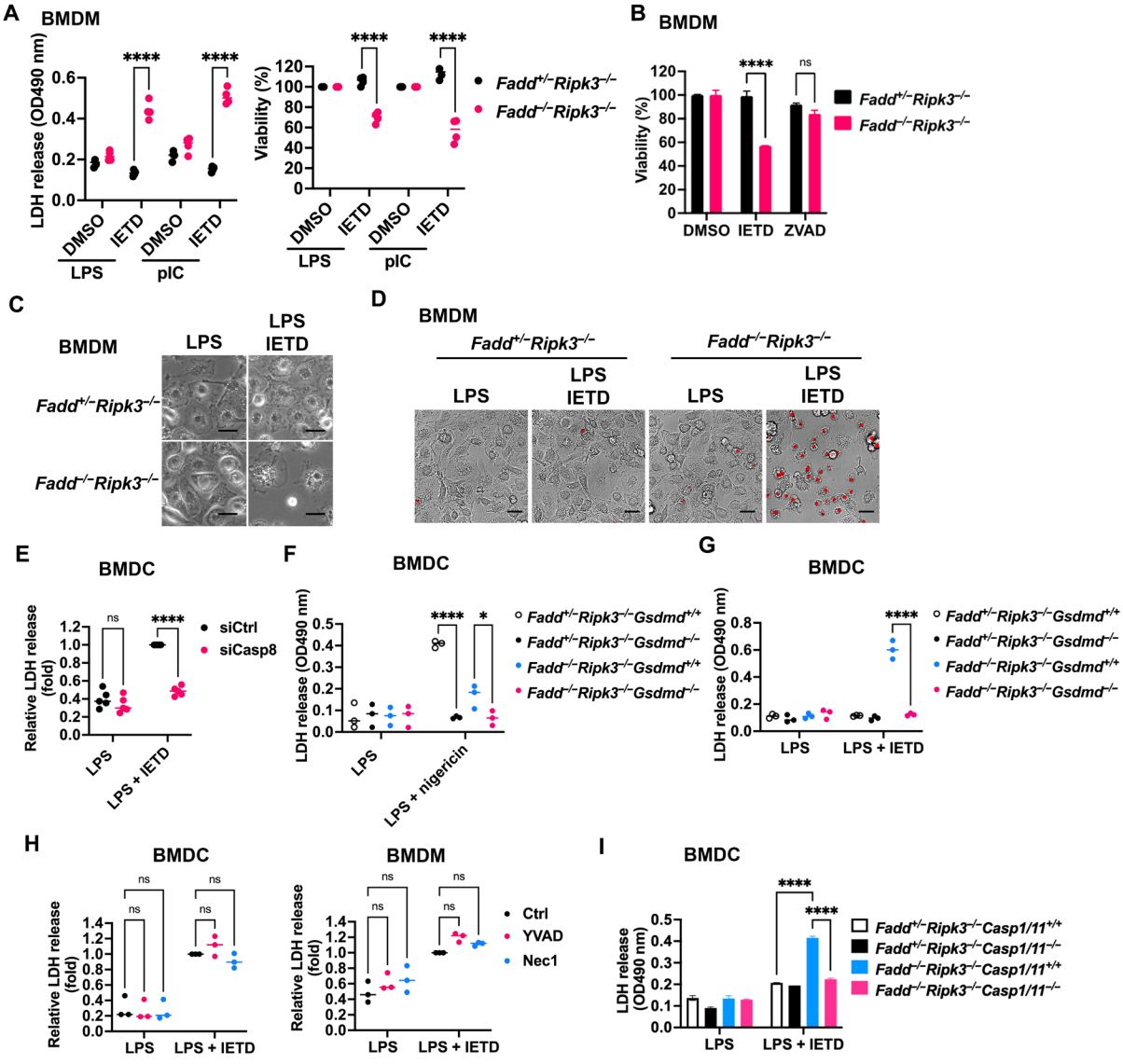

Fig. 5. IETD induces caspase-8–, caspase-1/11–, and GSDMD-dependent cell death in *Fadd*$^{-/-}$*Ripk3*$^{-/-}$ myeloid cells. (**A**) BMDMs were stimulated with LPS (0.1 μg/ml) or poly(I:C) (50 μg/ml) plus IETD (10 μM) for 20 hours. LDH release and cell viability (determined by ATP assay) were analyzed. (**B**) BMDMs were stimulated with LPS plus IETD or zVAD (40 μM) for 16 hours, and cell viability was analyzed. (**C** and **D**) BMDMs were stimulated with LPS with or without IETD, in the absence (C) or presence of PI (D), for 16 hours. Scale bars, 25 μm (C) and 50 μm (D). Bright-field images are representative of three independent experiments. (**E**) *Fadd*$^{-/-}$*Ripk3*$^{-/-}$ BMDCs were transfected with control or caspase-8 siRNA for 24 hours, followed by LPS + IETD treatment for 8 hours, and LDH release was determined. (**F** and **G**) LDH release from BMDCs of indicated *Gsdmd* genotypes upon treatment with LPS + nigericin for 20 min (F) or with LPS + IETD for 8 hours (G). (**H**) *Fadd*$^{-/-}$*Ripk3*$^{-/-}$ BMDCs and BMDMs were stimulated with LPS + IETD without or with YVAD (20 μM) or Nec-1 (40 μM) for 18 hours, and then LDH release was determined. (**I**) BMDCs of indicated *Casp1/11* genotypes were treated with LPS or LPS + IETD for 7.5 hours, and LDH release was quantified. Data represent four (A), five (E), and three (F to H) independent experiments, and mean values are indicated. For (B) and (I), data represent means ± SD of technical triplicates of an experiment representative of three independent experiments. *$P < 0.05$, **$P < 0.01$, ***$P < 0.001$, and ****$P < 0.0001$ for two-way ANOVA followed by Sidak's multiple comparisons test. ns, not significant.

3-methyladenine (3-MA) suppressed LPS + IETD–induced cell death in *Fadd*$^{-/-}$*Ripk3*$^{-/-}$ myeloid cells (Fig. 7, A and B). Next, we used the autophagy-specific fluorescence dye DAPGreen to characterize LPS + IETD–induced cell death. DAPGreen signal was absent from *Fadd*$^{-/-}$*Ripk3*$^{-/-}$ BMDMs stimulated with LPS alone but became abundant upon LPS + IETD treatment (Fig. 7C). Moreover, intracellular vesicles colocalized with DAPGreen signal in dying *Fadd*$^{-/-}$*Ripk3*$^{-/-}$ BMDMs (Fig. 7C). In contrast, we did not detect DAPGreen signals upon treatment with other stimuli, including necroptosis induction (LPS + zVAD), canonical inflammasome activation (LPS + nigericin), and intrinsic apoptosis (dexamethasone) (fig. S9), evidencing the specificity of DAPGreen signal. For LPS + IETD–treated *Fadd*$^{-/-}$*Ripk3*$^{-/-}$ BMDMs monitored under time-lapse fluorescence microscopy, the appearance of DAPGreen signal was immediately followed by PI^{+} signal (movies S1 and S2). 3-MA significantly inhibited the DAPGreen signals induced by LPS + IETD in *Fadd*$^{-/-}$*Ripk3*$^{-/-}$ BMDMs (Fig. 7D), revealing that deficiency of both FADD and RIPK3 leads to autophagy-dependent cell death upon stimulation with LPS + IETD.

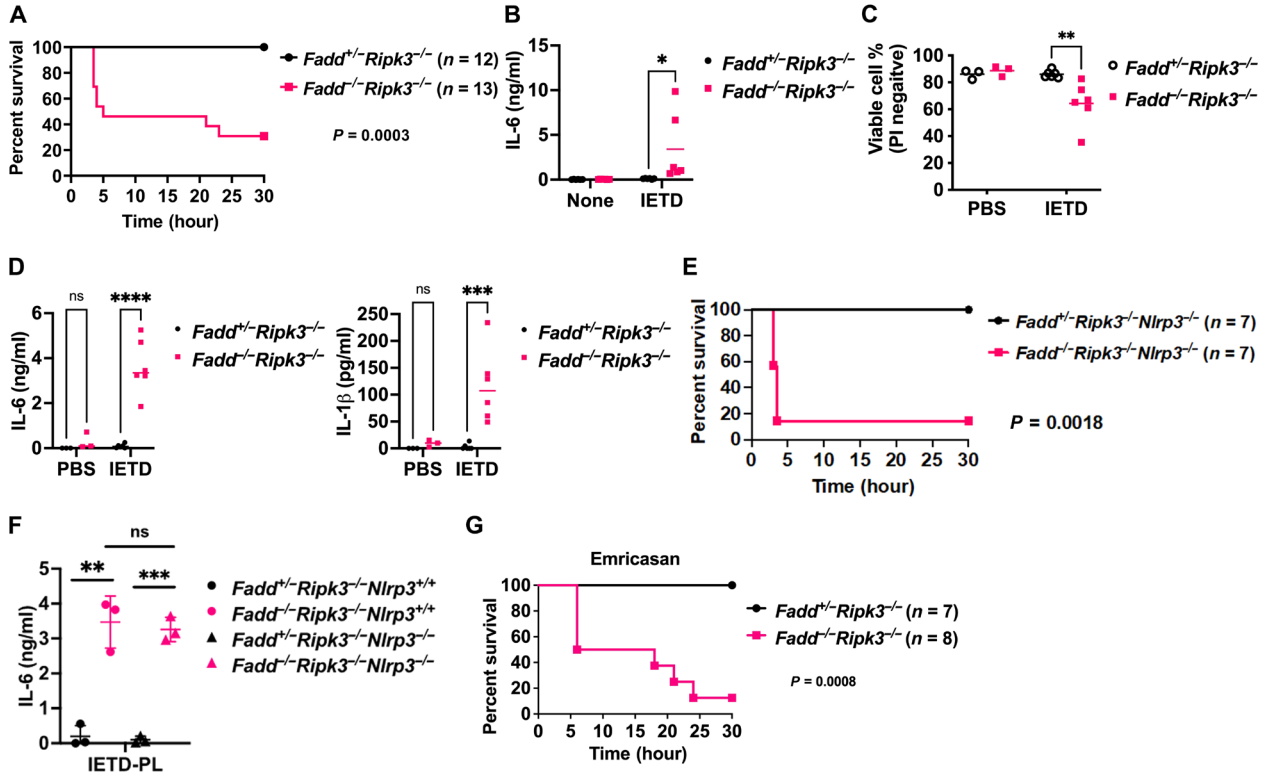

Fig. 6. IETD induces NLRP3-independent septic shock in *Fadd*$^{-/-}$*Ripk3*$^{-/-}$ mice. (**A**) Age- and sex-matched *Fadd*$^{+/-}$*Ripk3*$^{-/-}$ and *Fadd*$^{-/-}$*Ripk3*$^{-/-}$ mice were intraperitoneally injected with IETD (5 mg/kg), and then survival was determined at the indicated time points. The *P* value was determined by a log-rank (Mantel-Cox) test. (**B**) Serum concentration of IL-6 in mice before and 3 hours after IETD administration. $n = 3$ (control) and $n = 6$ (IETD). (**C**) Peritoneal cells were isolated from mice 3 hours after PBS or IETD administration. Viability was assessed by means of PI staining and quantitated by flow cytometry. Data are mean values for the PBS group ($n = 3$) or IETD group ($n = 6$). (**D**) Peritoneal cells were isolated from mice 3 hours after PBS or IETD administration, before determining levels of IL-6 and IL-1β. Data are mean values from $n = 3$ (PBS) and $n = 6$ (IETD). (**E**) *Fadd*$^{+/-}$*Ripk3*$^{-/-}$*Nlrp3*$^{-/-}$ and *Fadd*$^{-/-}$*Ripk3*$^{-/-}$*Nlrp3*$^{-/-}$ mice were administered with IETD (5 mg/kg) before determining survival ($n = 7$ for each group). The *P* value was determined by a log-rank (Mantel Cox) test. (**F**) Peritoneal cells were isolated from mice 3 hours after PBS or IETD administration, and then their production of IL-6 was determined ($n = 3$ for each group). (**G**) Emricasan (20 mg/kg) was administered to *Fadd*$^{+/-}$*Ripk3*$^{-/-}$ ($n = 7$) and *Fadd*$^{-/-}$*Ripk3*$^{-/-}$ ($n = 6$) mice, before determining mouse survival. The *P* value was determined by a log-rank (Mantel-Cox) test. (B to D and F) $^{*}P < 0.05$, $^{**}P < 0.01$, $^{***}P < 0.001$, and $^{****}P < 0.0001$ for two-way ANOVA followed by a Sidak's multiple comparison test.

Our results illustrated in Fig. 7 demonstrate that 3-MA inhibited LPS + IETD–induced cell death in *Fadd*$^{-/-}$*Ripk3*$^{-/-}$ myeloid cells. Autophagy involves fusion of autophagosomes with lysosomes, followed by excessive autolysosome formation. We examined whether the lysosome fusion inhibitor chloroquine or ammonium chloride blocked inflammasome activation as effectively as 3-MA in *Fadd*$^{-/-}$*Ripk3*$^{-/-}$ BMDMs. Similar to 3-MA, both chloroquine and ammonium chloride inhibited LPS + IETD–induced IL-1β or IL-18 production by *Fadd*$^{-/-}$*Ripk3*$^{-/-}$ BMDMs and BMDCs (Fig. 8, A and B). Both lysosome fusion inhibitors also inhibited LPS + IETD–induced cell death (Fig. 8C). A recent study has shown that histone deacetylase 6 (HDAC6) and microtubule assembly are required for NLRP3 inflammasome activation (*34*). Accordingly, we assessed whether the HDAC6 inhibitor tubacin or the tubulin polymerization inhibitor colchicine affected LPS + IETD–induced IL-18 production and cell death. However, neither tubacin nor colchicine had an impact on either parameter (fig. S10, A and B). 3-MA inhibited the generation of p20 caspase-1, p17 IL-1β, and GSDMD-NT induced by LPS + IETD in *Fadd*$^{-/-}$*Ripk3*$^{-/-}$ BMDCs, although 3-MA treatment modestly enhanced the expression of pro–IL-1β (Fig. 8D). LPS + IETD treatment also induced cleavage of caspase-3 in *Fadd*$^{-/-}$*Ripk3*$^{-/-}$ BMDMs (Fig. 8E), similar to observations in MLKL-deficient mice expressing inactive caspase-8 (*7*), and caspase-3 processing was inhibited by 3-MA (Fig. 8E). Notably, the caspase-3 inhibitor DEVD did not interfere with the IL-18 production and cell death induced by LPS + IETD (fig. S10, C and D). Neither did knockdown of caspase-3 nor caspase-7 affect inflammasome activation and cell death triggered by LPS + IETD (fig. S10E). We further knocked down Atg-5 in *Fadd*$^{-/-}$*Ripk3*$^{-/-}$ BMDCs and observed a reduction in IETD-triggered IL-1β production (Fig. 8, F and G). Atg-5 down-regulation also reduced IETD-induced cell death in *Fadd*$^{-/-}$*Ripk3*$^{-/-}$ BMDCs (Fig. 8G). Similarly, Beclin-1 knockout in *Fadd*$^{-/-}$*Ripk3*$^{-/-}$ BMDMs (Fig. 8H) reduced IETD-triggered IL-1β production and partially rescued *Fadd*$^{-/-}$*Ripk3*$^{-/-}$ BMDMs from IETD-induced cell death (Fig. 8I). Together, these results indicate that caspase-8 inactivation induces autophagy- and ASC-dependent, yet NLRP3-independent, inflammasome activation in *Fadd*$^{-/-}$*Ripk3*$^{-/-}$ myeloid cells.

IETD-induced septic shock in *Fadd*$^{-/-}$*Ripk3*$^{-/-}$ mice is independent of GSDMD and autophagy

We then examined whether IETD-induced septic shock involved IL-1β/IL-18, caspase-1/11, GSDMD, or autophagy. Administration

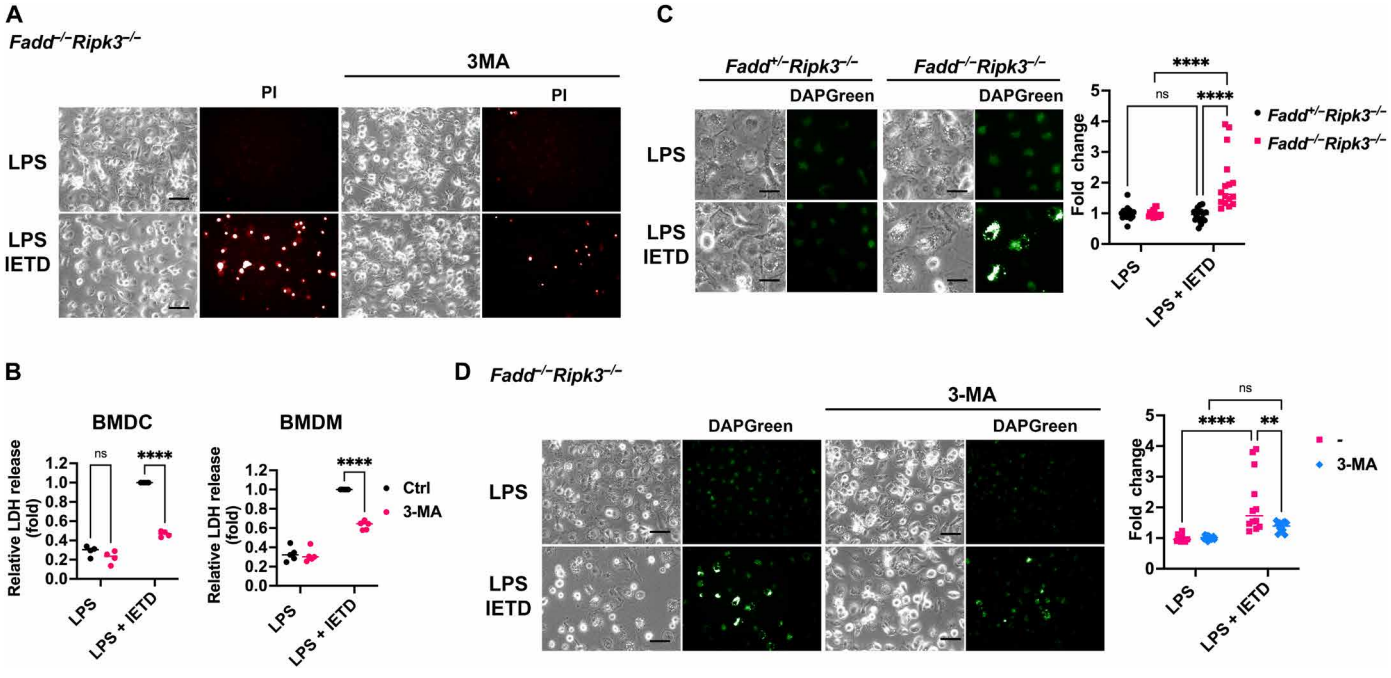

Fig. 7. Involvement of autophagy in IETD-induced cell death in *Fadd*$^{-/-}$*Ripk3*$^{-/-}$ myeloid cells. (**A**) Bright-field and PI staining images of BMDMs stimulated by LPS + IETD in the presence of 3-MA. *Fadd*$^{-/-}$*Ripk3*$^{-/-}$ BMDMs were treated with LPS (0.1 μg/ml) + IETD (10 μM) in the absence or presence of 3-MA (1 mM) for 18 hours. Images are representative of three independent experiments. Scale bar, 50 μm. (**B**) 3-MA inhibits IETD-induced cell death in *Fadd*$^{-/-}$*Ripk3*$^{-/-}$ myeloid cells. *Fadd*$^{-/-}$*Ripk3*$^{-/-}$ BMDCs and BMDMs were stimulated with LPS + IETD in the absence or presence of 3-MA (1 mM) for 8 hours (BMDCs) or 18 hours (BMDMs), and then LDH release was determined. LDH released from Ctrl cells treated with LPS + IETD was set as 1. Data represent mean values of four independent experiments. (**C**) Immunofluorescence analysis of DAPGreen in *Fadd*$^{-/-}$*Ripk3*$^{-/-}$ BMDMs. BMDMs were stained with DAPGreen (0.2 μM) for 30 min and then stimulated with LPS (0.1 μg/ml) plus IETD (10 μM) for 16 hours. Cell nuclei were stained with Hoechst 33342 Ready Flow reagent. Scale bar, 25 μm. Images are representative of four independent experiments. Average DAPGreen fluorescence intensity in a cell was quantified in ImageJ. The fluorescence intensity induced by LPS + IETD was compared to that of LPS alone. (**D**) 3-MA inhibits IETD-induced autophagy in *Fadd*$^{-/-}$*Ripk3*$^{-/-}$ BMDMs. *Fadd*$^{-/-}$*Ripk3*$^{-/-}$ BMDMs were stained with DAPGreen and stimulated with LPS + IETD as in (C), in the absence or presence of 3-MA (1 mM) for 16 hours. Images are representative of four independent experiments. Scale bar, 50 μm. Images were quantified as in (C). *P < 0.05, **P < 0.01, and ****P < 0.0001 for two-way ANOVA followed by Sidak's (B) or Tukey's (C and D) multiple comparisons test.

of anti–IL-1β and anti–IL-18 did not prevent the lethality of *Fadd*$^{-/-}$*Ripk3*$^{-/-}$ mice induced by IETD (fig. S11A), and application of disulfiram had no effect on the IETD-induced septic shock displayed by *Fadd*$^{-/-}$*Ripk3*$^{-/-}$ mice (fig. S11B). In addition, deletion of caspase-1 and caspase-11 failed to rescue *Fadd*$^{-/-}$*Ripk3*$^{-/-}$ mice from IETD-induced death (fig. S11C). GSDMD knockout also did not prevent *Fadd*$^{-/-}$*Ripk3*$^{-/-}$ mice from IETD-mediated death (fig. S11D). Neither did inhibition of autophagy by 3-MA confer resistance to IETD on *Fadd*$^{-/-}$*Ripk3*$^{-/-}$ mice (fig. S11E). Since systemic Beclin-1 deletion is embryonically lethal, we used *Fadd*$^{-/-}$*Ripk3*$^{-/-}$ *Becn1*$^{f/f}$*LysM*^{Cre} mice to determine their susceptibility to IETD. Beclin-1 deficiency in myeloid cells did not prevent IETD-triggered septic shock in *Fadd*$^{-/-}$*Ripk3*$^{-/-}$ mice (fig. S11F). Therefore, the processes involved in IETD-induced inflammasome activation in *Fadd*$^{-/-}$*Ripk3*$^{-/-}$ myeloid cells alone cannot account for the systemically lethal effect of IETD in *Fadd*$^{-/-}$*Ripk3*$^{-/-}$ mice. Although caspase-1/11, autophagy, and GSDMD mediate pyroptosis in IETD-stimulated *Fadd*$^{-/-}$*Ripk3*$^{-/-}$ myeloid cells, they are likely dispensable for the death of other cell types in IETD-treated *Fadd*$^{-/-}$*Ripk3*$^{-/-}$ mice.

One cell type potentially vulnerable to caspase-8 inactivation is intestinal epithelial cells (IECs) (*7*, *8*), so we determined the effect of IETD on those cells. Stimulation with LPS + IETD led to elevated cell death in *Fadd*$^{-/-}$*Ripk3*$^{-/-}$ IECs (fig. S12A). Moreover, treatment of *Fadd*$^{-/-}$*Ripk3*$^{-/-}$ IECs with zVAD or 3-MA did not prevent IETD-induced cell death (fig. S12B), suggesting that IECs are distinct from myeloid cells in terms of the involvement of autophagy in inflammasome activation following IETD treatment.

Cathepsin-B mediates IETD-induced inflammasome activation in *Fadd*$^{-/-}$*Ripk3*$^{-/-}$ myeloid cells

Although we found that IETD induced autophagy and inflammasome-associated pyroptosis in *Fadd*$^{-/-}$*Ripk3*$^{-/-}$ myeloid cells, the exact identities of the intermediate caspases/proteases activated by IETD remained obscure. Thus, first, we determined whether inhibition of other caspases mimicked the effect of IETD on *Fadd*$^{-/-}$*Ripk3*$^{-/-}$ myeloid cells. To do so, *Fadd*$^{-/-}$*Ripk3*$^{-/-}$ macrophages were stimulated with LPS plus various caspase inhibitors. In contrast to IETD, caspase inhibitors including VDVAD, VX-765, QVD, and zVAD all failed to stimulate IL-1β expression and induce cell death in LPS-primed *Fadd*$^{-/-}$*Ripk3*$^{-/-}$ BMDCs (fig. S13, A and B). Therefore, inhibition of other caspase did not reproduce the effect of IETD on *Fadd*$^{-/-}$*Ripk3*$^{-/-}$ myeloid cells.

Notably, pan-caspase inhibitor zVAD and QVD did not trigger inflammasome activation and cell death despite suppression of caspase-8 in *Fadd*$^{-/-}$*Ripk3*$^{-/-}$ myeloid cells, suggesting that inhibition of caspase-8 by IETD induces another caspase/protease that is also suppressed by zVAD or QVD. This scenario was also illustrated by the IL-1β production and cell death induced by LPS + IETD

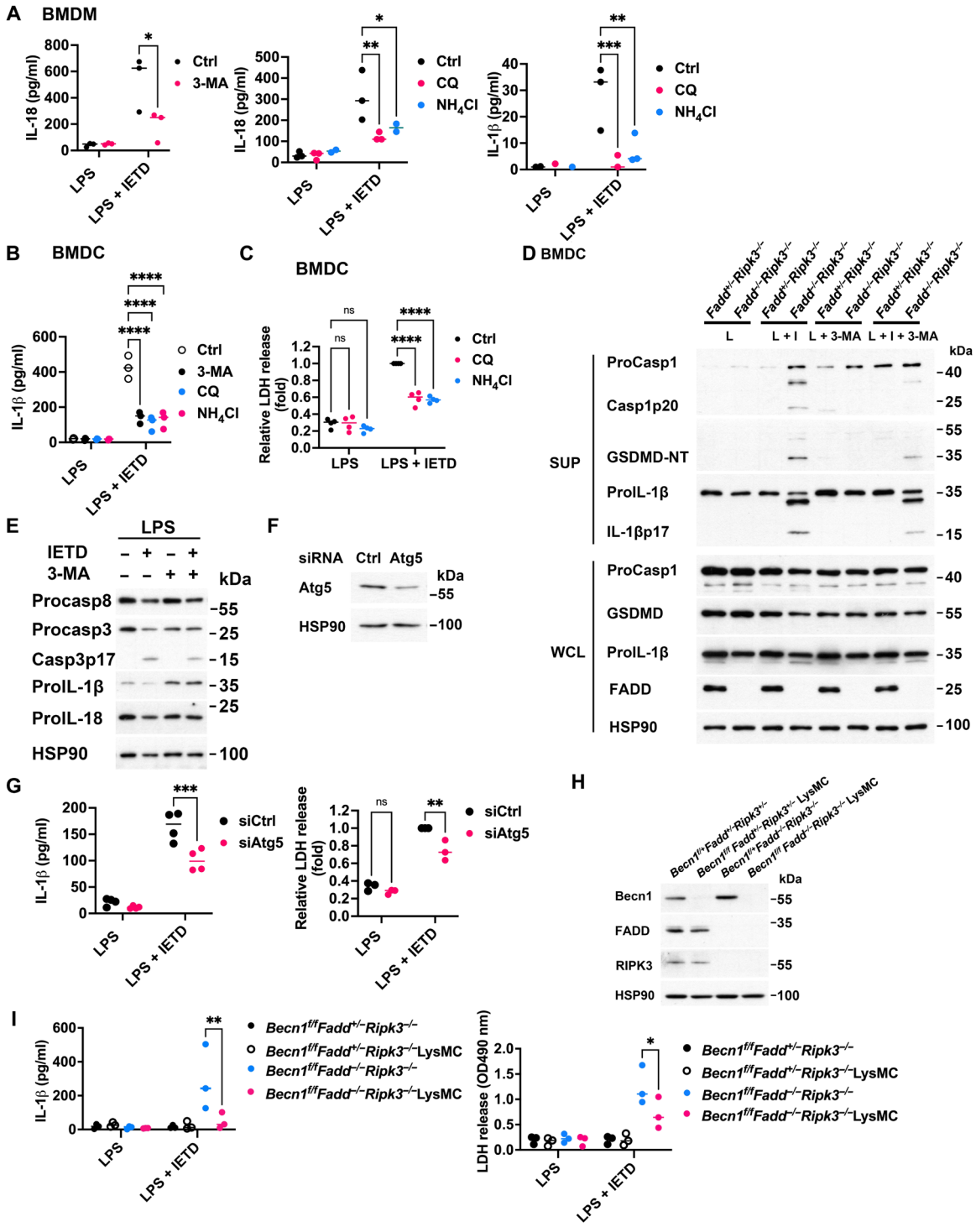

Fig. 8. Inhibition of autophagy attenuates IETD-induced inflammasome activation in *Fadd*$^{-/-}$*Ripk3*$^{-/-}$ myeloid cells. (**A** to **C**) *Fadd*$^{-/-}$*Ripk3*$^{-/-}$ BMDMs (A) and BMDCs (B and C) were stimulated with LPS (0.1 μg/ml) plus IETD (10 μM) in the absence (Ctrl) or presence of 3-MA (1 mM), chloroquine (10 μM), or NH_4Cl (2 mM) for 18 hours (A) or 8 hours (B and C); then IL-1β (A, B) and IL-18 (A) levels were determined; and LDH release (C) was quantitated. (**D** and **E**) *Fadd*$^{-/-}$*Ripk3*$^{-/-}$ BMDCs were treated with LPS, IETD, or 3-MA as indicated. Culture supernatants (D) and whole-cell lysates (D and E) were analyzed for inflammasome effectors. Results are representative of three independent experiments. (**F** and **G**) *Fadd*$^{-/-}$*Ripk3*$^{-/-}$ BMDCs were transfected with control or Atg-5–specific siRNAs for 24 hours, and then Atg5 contents were determined (F). Cells were then treated with LPS + IETD for 8 hours, before determining IL-1β production (G, left panel) and LDH release (G, right panel). (**H**) Beclin-1, RIPK3, and FADD contents in BMDMs of indicated *Becn1* genotypes were determined. (**I**) BMDMs were treated with LPS (0.1 μg/ml) + IETD (10 μM) for 18 hours, and then IL-1β levels were determined by ELISA (upper panel). LDH release was quantitated (lower panel). Data represent three [A, B, G (LDH), and I] or four [C and G (IL-1β)] independent experiments, and mean values are indicated. *$P < 0.05$, **$P < 0.01$, ***$P < 0.001$, and ****$P < 0.0001$ for two-way ANOVA followed by a Sidak's multiple comparison test.

being fully suppressed by zVAD in *Fadd*$^{-/-}$*Ripk3*$^{-/-}$ BMDCs and BMDMs (fig. S14, A to D). IETD-induced IL-1β production and cell death could also be partially inhibited by QVD in *Fadd*$^{-/-}$*Ripk3*$^{-/-}$ BMDMs (fig. S14, C and D). Next, we explored potential activation of other caspases/proteases upon IETD treatment in *Fadd*$^{-/-}$*Ripk3*$^{-/-}$ myeloid cells. We already found that caspase-1, caspase-3, or caspase-7 alone was dispensable for IETD-induced inflammasome activation in *Fadd*$^{-/-}$*Ripk3*$^{-/-}$ myeloid cells (Fig. 3C and fig. S10, C to E). Inclusion of inhibitors for caspase-2 (VDVAD), caspase-6 (VEID), or caspse-9 (LEHD) did not prevent IETD-triggered IL-1β production and cell death (fig. S14). In searching for other proteases that may account for the effect of IETD in *Fadd*$^{-/-}$*Ripk3*$^{-/-}$ myeloid cells, we found that the cathepsin-B inhibitor CA-074Me suppressed IETD-induced IL-1β production (Fig. 9A). CA-074Me also prevented IETD-triggered cell death in *Fadd*$^{-/-}$*Ripk3*$^{-/-}$ BMDCs (Fig. 9B). However, no effect was detected when the cathepsin-D inhibitor pepstatin A was included (Fig. 9, A and B). Cathepsin-B is known to be suppressed by zVAD (*35*), implying that the effectiveness of zVAD in antagonizing IETD activity (fig. S14) could be due to targeting cathepsin-B. To further verify the role of cathepsin-B in LPS + IETD–induced inflammasome activation, we down-regulated cathepsin-B by means of specific small interfering RNAs (siRNAs) (Fig. 9C). Cathepsin-B knockdown reduced IETD-triggered IL-1β production in *Fadd*$^{-/-}$*Ripk3*$^{-/-}$ dendritic cells (Fig. 9D). Given that cathepsin-B is known to cleave caspase-11 and participates in inflammasome activation (*36*–*38*), we found that CA-074Me inhibited the cleavage of caspase-1, GSDMD, and IL-1β (Fig. 9E). In contrast, CA-074Me did not protect *Fadd*$^{-/-}$*Ripk3*$^{-/-}$ IECs from IETD-induced cell death (fig. S12C). Neither did CA-074Me confer resistance of *Fadd*$^{-/-}$*Ripk3*$^{-/-}$ mice to IETD-mediated septic shock (fig. S11G). Therefore, our results imply that, at least in part, cathepsin-B accounts for IETD-induced inflammasome activation in *Fadd*$^{-/-}$*Ripk3*$^{-/-}$ myeloid cells.

Overall, then, our findings provide evidence that autophagy and cathepsin-B represent one of the intermediate stages between caspase-8 inactivation, inflammasome formation, and the cell death triggered by caspase-8 inactivation in myeloid cells when apoptosis and necroptosis are blocked (fig. S15). Upon caspase-8 inactivation by IETD, caspase-8 becomes associated with ASC, the complex induces autophagy, and the autophagosome becomes accessible to cathepsin-B, enabling atypical inflammasome formation for activation of caspase-1/11. Caspase-1 processes IL-1β/IL-18, and caspase-1/11 cleave GSDMD. Cathepsin-B also directly activates caspase-11. Thus, together, our results reveal a novel process by which caspase-8 inactivation leads to atypical inflammasome activation in myeloid cells deficient in apoptosis and necroptosis.

DISCUSSION

Caspase-8 is well known for its various roles in controlling apoptosis, necroptosis, and pyroptosis. In this study, we uncovered an unconventional function for caspase-8 in mediating inflammasome activation and cell death in myeloid cells deficient in both FADD and RIPK3. Administration of IETD into the peritoneum of *Fadd*$^{-/-}$*Ripk3*$^{-/-}$ mice resulted in inflammatory cytokine production and mortality within hours. We have further identified that IETD could trigger autophagy in *Fadd*$^{-/-}$*Ripk3*$^{-/-}$ myeloid cells. Inhibition of autophagy partially suppressed IETD-induced IL-1β/IL-18 production and cell death in these cells. Suppression of cathepsin-B also inhibited IETD-triggered inflammasome activation in *Fadd*$^{-/-}$*Ripk3*$^{-/-}$ myeloid cells. Our results suggest that autophagy and cathepsin-B activity represent intermediate steps between the caspase-8 inactivation, inflammasome formation, and cell death in myeloid cells in which apoptosis and necroptosis are blocked.

We have demonstrated that caspase-8 protein is required for IETD-induced atypical inflammasome activation in *Fadd*$^{-/-}$*Ripk3*$^{-/-}$ myeloid cells. Knockdown of caspase-8 abolished the ability of IETD to induce IL-1β production and cell death in *Fadd*$^{-/-}$*Ripk3*$^{-/-}$ BMDCs stimulated with LPS (Figs. 3B and 5E), indicating that the presence of inactivated caspase-8 is indispensable for inflammasome activation. Therefore, IL-1β and IL-18 generation is not an off-target effect of IETD in *Fadd*$^{-/-}$*Ripk3*$^{-/-}$ cells. Instead, inactive caspase-8 likely serves as a scaffold protein to trigger inflammasome assembly in those cells, which is supported by studies showing that inactivated caspase-8 adopts a conformation distinct from active caspase-8 and that the former nucleates ASC for subsequent caspase-1 activation (*7*). We also observed ASC dimerization in response to either R848 + IETD or LPS + nigericin treatment in *Fadd*$^{-/-}$*Ripk3*$^{-/-}$ BMDCs (Fig. 2D). We found that NLRP3 was dispensable for IETD-triggered inflammasome activation in *Fadd*$^{-/-}$*Ripk3*$^{-/-}$ myeloid cells, as revealed by their normal production of IL-1β and IL-18 (fig. S7, B and C). Consistent with previous reports that caspase-8 inactivation triggers pyroptosis when apoptosis and necroptosis are inhibited (*7*, *8*), we found that GSDMD contributed to death in IETD-treated *Fadd*$^{-/-}$*Ripk3*$^{-/-}$ myeloid cells. GSDMD knockout interfered with IETD-induced death in those cells (Fig. 5G), and we detected a striking inhibitory effect of GSDMD knockout or disulfiram treatment on IETD-triggered IL-1β/IL-18 production (Fig. 4, B, C, E, and F).

Among the downstream targets of caspase-8, RIPK1 is cleaved by caspase-8 at D324 and D325 to limit apoptosis and necroptosis (*39*–*41*). It has been shown previously that noncleavable RIPK1 mutants contribute to autoinflammatory disease by enhancing RIPK1-mediated apoptosis and necroptosis (*33*, *39*, *42*). Knockout of RIPK3 abrogates cell death in cells harboring these noncleavable RIPK1 mutants (*33*, *39*). Intriguingly, cells are extremely sensitive to the TNF-induced cell death that is inhibited by Nec-1 or a RIPK1 inactive mutant resistant to caspase-8 cleavage (*33*, *42*). We found that Nec-1 treatment did not prevent IETD-induced cell death in *Fadd*$^{-/-}$*Ripk3*$^{-/-}$ myeloid cells (Fig. 5H). In addition, RIPK1 levels were reduced in *Fadd*$^{-/-}$*Ripk3*$^{-/-}$ cells relative to control cells (fig. S5A). Together, these findings indicate that the cell death induced by IETD in *Fadd*$^{-/-}$*Ripk3*$^{-/-}$ myeloid cells is unlikely to be mediated by the excess presence of an uncleavable form of RIPK1.

We also observed that the IETD-induced IL-1β/IL-18 production in *Fadd*$^{-/-}$*Ripk3*$^{-/-}$ cells cannot be recapitulated by replacing IETD with zVAD, supporting that specific inhibition of caspase-8 protease activity is essential. One potential reason for the differential outcomes for IETD and zVAD treatment is that IETD-induced inflammasome activation also activates other caspases that are essential for generating IL-1β/IL-18, with the pan-caspase inhibitor zVAD blocking all these processes. A recent study has revealed that processing of caspase-3 and caspase-7 by caspase-1 is inhibited in cells in which apoptosis and necroptosis are suppressed (*7*). We also detected caspase-3 cleavage in *Fadd*$^{-/-}$*Ripk3*$^{-/-}$ myeloid cells treated with IETD + LPS (Fig. 7E), but neither a caspase-1 inhibitor nor a caspase-3 inhibitor prevented IETD-induced inflammasome activation in those cells (Fig. 3, C and D, and fig. S10, C and D). Similarly, knockdown

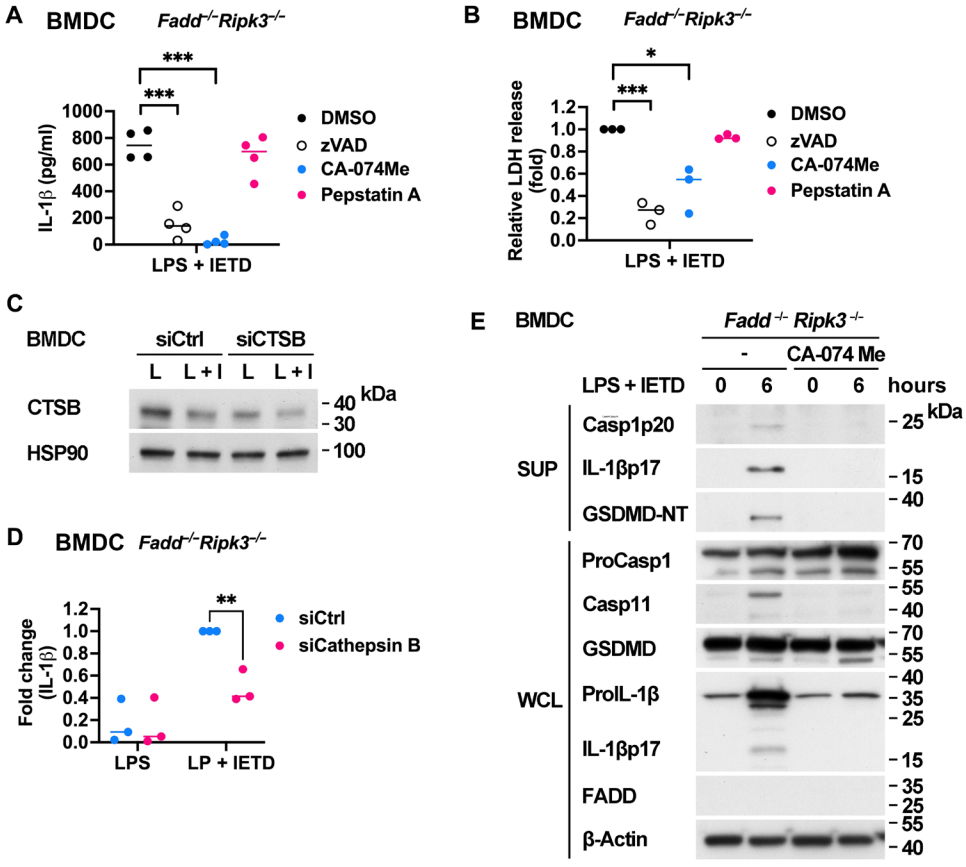

Fig. 9. Cathepsin-B mediates the inflammasome activation and caspase cleavage induced by IETD in *Fadd*$^{-/-}$*Ripk3*$^{-/-}$ myeloid cells. (**A** and **B**) A cathepsin-B inhibitor suppresses IETD-induced IL-1β generation and cell death in *Fadd*$^{-/-}$*Ripk3*$^{-/-}$ BMDCs. *Fadd*$^{+/-}$*Ripk3*$^{-/-}$ and *Fadd*$^{-/-}$*Ripk3*$^{-/-}$ BMDCs were stimulated with LPS (0.1 μg/ml) + IETD (15 μM) in the presence of CA-074Me (50 μM) or pepstatin A (50 μM, a cathepsin-D inhibitor) for 8 hours. IL-1β production was determined (A), and cell death (as assessed by LDH release) was quantified (B). *$P < 0.05$ and ***$P < 0.001$ for unpaired *t* test. (**C** and **D**) Cathepsin-B knockdown reduces IETD-induced IL-1β in *Fadd*$^{-/-}$*Ripk3*$^{-/-}$ BMDCs. *Fadd*$^{-/-}$*Ripk3*$^{-/-}$ BMDCs were transfected with control or cathepsin-B–specific siRNAs, before determining cathepsin-B levels (C). Cells were then treated with LPS (0.1 μg/ml) + IETD (10 μM) for 8 hours, before IL-1β production was quantitated (D). **$P < 0.01$ for two-way ANOVA followed by Sidak's multiple comparisons test. (**E**) Inhibition of cathepsin-B prevents IETD-triggered caspase-1/11 and GSDMD processing in *Fadd*$^{-/-}$*Ripk3*$^{-/-}$ BMDCs. BMDCs were stimulated with LPS (0.1 μg/ml) plus IETD (10 μM) for 6 hours. Culture supernatants (SUP) were precipitated, and whole-cell lysates (WCL) were collected and analyzed for caspase-1 p20, IL-1β p17, GSDMD-NT, procaspase-1, caspase-11, GSDMD, and pro–IL-1β. The experiment (E) was independently repeated three times with similar results.

of caspase-3 or caspase-7 failed to inhibit IL-1β production and cell death in IETD-treated *Fadd*$^{-/-}$*Ripk3*$^{-/-}$ BMDCs (fig. S10E). We also found that inclusion of inhibitors for caspase-2, caspase-6, and caspase-9 did not prevent IETD-initiated inflammasome activation (fig. S14). Thus, the executer of IL-18 and IL-1β processing in IETD-treated *Fadd*$^{-/-}$*Ripk3*$^{-/-}$ myeloid cells is likely not a single commonly known caspase.

An important finding of our study is the identification of autophagy as an upstream process for inflammasome activation and cell death in IETD-treated *Fadd*$^{-/-}$*Ripk3*$^{-/-}$ myeloid cells. Autophagy is well known for its inhibitory role in canonical NLRP3 inflammasome formation (*34*, *43*, *44*). Accordingly, our discovery that autophagy mediates an element of caspase-8 inactivation–induced inflammasome activation in *Fadd*$^{-/-}$*Ripk3*$^{-/-}$ myeloid cells is unexpected. We observed high-intensity signal of the autophagy-specific dye DAPGreen in the spherical vesicles induced by LPS + IETD treatment of *Fadd*$^{-/-}$*Ripk3*$^{-/-}$ cells (Fig. 7 and movie S2), but not in WT cells undergoing apoptosis, necroptosis, or conventional pyroptosis (fig. S9). Moreover, 3-MA, chloroquine, and ammonium chloride inhibited LPS + IETD–induced IL-1β and IL-18 production in *Fadd*$^{-/-}$*Ripk3*$^{-/-}$ cells (Fig. 8, A and B). This outcome is further supported by the suppression by 3-MA of p20 caspase-1, p17 IL-1β, and GSDMD-NT processing in the same cells (Fig. 8D). 3-MA also inhibited caspase-3 cleavage in *Fadd*$^{-/-}$*Ripk3*$^{-/-}$ BMDMs (Fig. 8E). Moreover, we found that knockout of Beclin-1 attenuated IETD-triggered IL-1β production in such cells (Fig. 8I). Together, these results suggest that autophagy precedes assembly of the atypical inflammasome, and it is critical for inflammasome formation. In addition, since IETD-induced cell death in *Fadd*$^{-/-}$*Ripk3*$^{-/-}$ cells could be partially abrogated by 3-MA, chloroquine, or ammonium chloride treatments or Beclin-1 knockout (Fig. 8, C and I), autophagy also participates in the processes leading to cell death. Autophagy inhibition had more profound effects on IETD-induced IL-1β/IL-18 production than on IETD-triggered cell death in *Fadd*$^{-/-}$*Ripk3*$^{-/-}$ cells, implying that autophagy represents one of several processes contributing to cell death.

Previous studies have demonstrated cross-talk between caspase-8 and autophagy, given that caspase-8 cleaves Beclin-1 and Atg3 (*45*),

whereas inactivation of caspase-8 triggers autophagic cell death (*26*). However, there are important differences between those previous reports and our findings presented here. In contrast to how zVAD induces autophagy in L929 fibroblasts (*26*), we found that the effect of IETD treatment cannot be recapitulated by zVAD in terms of inflammasome activation (Fig. 3A). In addition, we found that IETD only induced cell death in *Fadd*$^{-/-}$*Ripk3*$^{-/-}$ myeloid cells, but not in *Fadd*$^{+/-}$*Ripk3*$^{-/-}$ cells, indicating a specific requirement for blockade of both apoptosis and necroptosis. Notably, p62 has been shown to promote caspase-8 aggregation on autophagosomes (*46*), potentially reflecting a process to initiate inflammasome formation. FADD suppresses noncleavable caspase-8–mediated ASC speck assembly (*20*). It is possible that the binding of inactivated caspase-8 to ASC or p62 is inhibited by caspase-8–interacting FADD, so competition between ASC/p62 and FADD for caspase-8 may explain why inactivated caspase-8 does not trigger inflammasome activation in FADD-sufficient cells.

Another novel finding from our study is the identification of a role for cathepsin-B in atypical inflammasome activation, as revealed by CA-074Me suppressing IETD-induced caspase-1 activation, GSDMD cleavage, p17 IL-1β generation, and cell death in *Fadd*$^{-/-}$*Ripk3*$^{-/-}$ BMDCs (Fig. 9, A, B, and E). This novel function is also supported by the fact that cathepsin-B knockdown reduced IL-1β generation in IETD-treated *Fadd*$^{-/-}$*Ripk3*$^{-/-}$ BMDCs (Fig. 9D). Cathepsin-B is suppressed by zVAD (*35*), consistent with our observation that IETD-triggered IL-1β/IL-18 expression and cell death were effectively inhibited by zVAD (fig. S14), and it explains the limited inflammasome activation elicited by LPS + zVAD treatment (figs. S2E and S13). Cathepsin-B binds NLRP3 to activate the NLRP3 inflammasome (*38*). It has also been shown to directly cleave and activate caspase-11 (*37*), which may contribute to the caspase-11 activation observed in the present study. Cathepsin-B also participates in the activation of caspase-1 and caspase-11, as well as IL-1β/IL-18 secretion in microglia independently of NLRP3 (*36*). In contrast to canonical inflammasome activation, lysosome destabilization is not involved in the initiation of this type of inflammation (*36*). Similar to those previous results, our observations suggest that cathepsin-B is the protease that mediates atypical inflammasome activation following NLRP3-indepdendent caspase-8 inactivation in *Fadd*$^{-/-}$*Ripk3*$^{-/-}$ myeloid cells.

We suggest that cathepsin-B acts downstream of autophagy. Our proposed scenario is that following autophagosome maturation or cytosolic entry of cathepsin-B, the caspase-8–ASC platform becomes accessible to cathepsin-B in *Fadd*$^{-/-}$*Ripk3*$^{-/-}$ myeloid cells (fig. S15). Cathepsin-B activity contributes to inflammasome activation, leading to activation of caspase-1 and caspase-11, processing of IL-1β/IL-18, and generation of GSDMD-M (Fig. 9E). Further studies are required to elucidate the exact sequence of biochemical and cellular steps from caspase-8 inactivation to autophagosome formation, followed by cathepsin-B association and atypical inflammasome assembly in *Fadd*$^{-/-}$*Ripk3*$^{-/-}$ myeloid cells. It should also be noted that residual IETD-mediated inflammasome activation was observed when we inhibited autophagy (Fig. 8, D, E, G, and I) or upon cathepsin-B suppression (Fig. 9, B and D), indicating that autophagy and cathepsin-B may not be the only pathway operating downstream of caspase-8 inactivation in *Fadd*$^{-/-}$*Ripk3*$^{-/-}$ myeloid cells. Identification of other parallel processes involved in atypical inflammasome activation in *Fadd*$^{-/-}$*Ripk3*$^{-/-}$ myeloid cells will help establish a complete picture of this unusual event.

One limitation of the present study is that the involvement of autophagy in IETD-induced inflammasome activation could be restricted to myeloid cells of the *Fadd*$^{-/-}$*Ripk3*$^{-/-}$ background. The capacity of caspase-8 and FADD to induce inflammasome activation is cell type specific (*20*, *22*). Here, we have found that autophagy inhibition, cathepsin-B deficiency, or GSDMD knockout impaired IETD-induced IL-1β/IL-18 production and cell death in *Fadd*$^{-/-}$*Ripk3*$^{-/-}$ myeloid cells. These outcomes contrast with the failure of 3-MA, CA-074-Me, or GSDMD knockout to rescue IETD-triggered lethality in *Fadd*$^{-/-}$*Ripk3*$^{-/-}$ mice. The discrepancy between our in vitro and in vivo findings could be due to the different cell types targeted. In scenarios where apoptosis, necroptosis, and pyroptosis are being genetically manipulated, mouse mortality is largely determined by nonimmune cells such as IECs (*4*–*8*, *33*, *47*). In contrast, our study focused on macrophages and dendritic cells in which phagocytosis and micropinocytosis predominate (*48*), potentially contributing to the dominant role of autophagy in assembly of atypical inflammasomes in those cells. We found that inhibition of autophagy or suppression of cathepsin-B did not prevent IETD-initiated cell death in *Fadd*$^{-/-}$*Ripk3*$^{-/-}$ IECs, implying that autophagy-independent processes operate in IECs and other cell types. Therefore, how caspase-8 inactivation triggers cell death in *Fadd*$^{-/-}$*Ripk3*$^{-/-}$ nonmyeloid cells, especially IECs, remains to be elucidated by future studies.

In summary, we have identified autophagy as one of the processes operating between caspase-8 inactivation and atypical inflammasome activation in myeloid cells in which apoptosis and necroptosis are blocked. Inhibition of autophagy prevents IL-1β/IL-18 generation and partially suppresses IETD-induced cell death in *Fadd*$^{-/-}$*Ripk3*$^{-/-}$ myeloid cells. Suppression of cathepsin-B also alleviates IETD-triggered atypical inflammasome activation. Thus, our results indicate that caspase-8 inactivation triggers autophagy and recruits cathepsin-B to dictate one of the molecular switches from apoptosis/necroptosis to pyroptosis in myeloid cells.

MATERIALS AND METHODS

Mice

Fadd$^{-/-}$*FADD:GFP*^{flox} mice were generated by J. Zhang (Thomas Jefferson University, Philadelphia, PA). The *Fadd*$^{-/-}$*FADD:GFP*^{flox} mice were bred with *LysM*^{Cre} mice (B6.129P2-*Lyz2*$^{tm1(cre)Ifo}$/J, #004781, The Jackson Laboratory, Bar Harbor, ME, USA) to generate *Fadd*$^{-/-}$*FADD:GFP*^{flox} *LysM*^{Cre} mice. *Gsdmd*$^{-/-}$ mice (C57BL/6J-*Gsdmd*^{em1Vnce}/J, #032663) (*49*), *Casp1/11*$^{-/-}$ mice (B6N.129S2-*Casp1*^{tm1Flv}/J, #016621), and *Becn1*^{flox} mice (*Becn1*$^{tm1.1Yue}$/J, #028794) were also obtained from The Jackson Laboratory. The *Becn1*^{flox} mice were bred with *LysM*^{Cre} mice to generate *Becn1*$^{f/f}$*LysM*^{Cre} mice. *Nlrp3*$^{-/-}$ mice were generated by B. Ruffle (Centre National de la Recherche Scientifique, France) and provided to us by D. Ojcius (Center for Molecular and Clinical Immunology, Chang Gung University, Taiwan). *Ripk3*$^{-/-}$ mice were generated by a CRISPR-Cas9 approach using the following sequences: single-guide RNA (sgRNA) target 1, 5′-GTCTGTGCACACATAACTCCAGG-3′; sgRNA target 2, 5′-ACAGGCCTAATGCACCCTCACGG-3′. RIPK3 genomic DNA typing was performed by polymerase chain reaction (PCR) using the following primers, RIPK3-fwd (5′-GGAGCCTCTTATTTGAAAGG-3′) and RIPK3-rev (5′-GACAGGCCAAAATCTGCTAG-3′), generating PCR products of 410 base pairs (bp) for the knockout allele or 1400 bp for the WT allele: RIPK3-I3F, 5′-GTTCCGGGCACACCACAGAA-3′; RIPK3-E4R,

5′-GCAGGAGCGGAGGGTTCAAG-3′. The *Ripk3*$^{-/-}$ mice were bred with *Fadd*$^{-/-}$*FADD:GFP*^{flox} mice to generate *Ripk3*$^{-/-}$*Fadd*$^{-/-}$ mice. PCR primers for WT FADD genomic DNA were FADDE1F (5′-CACTGCCATGGACCCATTCC-3′) and FADDE1R (5′-GCGCAGCGAGGCCAGCAACT-3′). For FADD-deleted genomic DNA, they were Neo41F (5′-CTTGGGTGGAGAGGCTATTC-3′) and Neo210R (5′-CAGCCACGATAGCCGCGCTG-3′). The phenotypes of *Ripk3*$^{-/-}$ *Fadd*$^{-/-}$ mice, characterized by lymphadenopathy and splenomegaly, were comparable to reports of other *Ripk3*$^{-/-}$ *Fadd*$^{-/-}$ mice (*47*). *Nlrp3*$^{-/-}$ mice, *Casp1/11*$^{-/-}$ mice, *Gsdmd*$^{-/-}$ mice, or *Becn1*$^{f/f}$*LysM*^{Cre} mice were further bred with *Fadd*$^{+/-}$*Ripk3*$^{-/-}$ or *Fadd*$^{-/-}$*Ripk3*$^{-/-}$ mice to generate mice strains for the present study. All mouse experiments were conducted with approval (protocol #17-12-1172) from the Institutional Animal Care and Utilization Committee, Academia Sinica.

PCR primers for WT *Nlrp3* genomic DNA were Nlrp3IntronF (5′-GCTCAGGACATACGTCTGGA-3′) and Nlrp3E1R (5′-CCTTGAAGATGTGGACCTCA-3′). For *Nlrp3*-deleted genomic DNA, they were Nlrp3IntronF and Nlrp3MutantR (5′- TTGTAGTTGCCGTCGTCCTT-3′). PCR primers for WT *Casp1/11* genomic DNA were mCasp1WTF (5′-GAGACATATAAGGGAGAAGGG-3′) and mCasp1ComR (5′-ATGGCACACCACAGATATCGG-3′). For *Casp1/11*-deleted genomic DNA, they were mCasp1MutF (5′-TGCTAAAGCGCATGCTCCAGACTG-3′) and mCasp1ComR. PCR primers for WT *Gsdmd* genomic DNA were mGsdmdSeqF (5′- GAACCATCTCTCCAGCCTGA-3′) and mGSDMDWTR (5′-ATGCCTGACAACATCAC-3′). For *Gsdmd*-deleted genomic DNA, they were mGsdmdSeqF and mGSDMDMutR (5′-CTCTGCATCCACACACCTT-3′). PCR primers for *Becn1 Flox* were mBecn1F (5′-TCTTCACCTCCACCACCAAG-3′) and mBecn1R (5′-CCCGGTCCAGGATCTTGAAG-3′).

Reagents and antibodies

Purified LPS, R848, poly(I:C), CpG, nigericin, and heat-killed *Candida albicans* were purchased from InvivoGen (San Diego, CA, USA). A TNF-α mouse ELISA kit, an IL-6 mouse ELISA kit, an IL-1β mouse ELISA kit, and Lipofectamine 2000 were purchased from Thermo Fisher Scientific (Waltham, MA, USA). Ac-YVAD-cmk, Nec-1, CHAPS, MG132, dexamethasone, chloroquine, tubacin, colchicine, 3-MA, and emricasan (SML2227) were all purchased from Sigma-Aldrich (St. Louis, MO). Dimethyl sulfoxide (DMSO) was purchased from Merck Millipore (Billerica, MA). Recombinant granulocyte-macrophage colony-stimulating factor (GM-CSF) was purchased from PeproTech (Rocky Hill, NJ, USA). Z-IETD-fmk was obtained from R&D Systems (Minneapolis, MN, USA), MedChemExpress (Monmouth Junction, NJ, USA), and Taiclone Biotech Corp. (Taipei, Taiwan). z-VAD-FMK was obtained from Bachem (Bubendorf, Switzerland). Q-VD-Oph and Ac-DEVD-CHO were obtained from CiteAb (Bath, UK). VX-765 and Z-VDVAD-FMK were purchased from BioVision (Milpitas, CA, USA). Z-VEID-FMK and Z-LEHD-FMK were purchased from Abcam (Cambridge, UK). CA-074Me was obtained from MedChemExpress. DAPGreen was purchased from Dojindo Molecular Technologies Inc. (Rockville, MD).

Anti-mouse RIPK3 (95702, RRID:AB_2721823), anti-pIKK (2078, RRID:AB_2079379), anti-IKKβ (8943, RRID:AB_11024092), anti-pJNK (9251, RRID:AB_331659), anti-JNK (9252, RRID:AB_2250373), anti-pp38 (9211, RRID:AB_331641), anti-p38 (9218, RRID:AB_10694846), anti-pERK (9101, RRID:AB_331646), anti-ERK(9102,RRID:AB_330744),anti-Atg5(12994,RRID:AB_2630393), anti–Beclin-1 (3495, RRID:AB_1903911), anti–caspase-3 (9662, RRID:AB_331439), anti–cleaved caspase-3 (9661, RRID:AB_2341188), anti-mouse caspase-8 (4927, RRID:AB_2068301), and anti–cleaved caspase-8 (9429, RRID:AB_2068300) were purchased from Cell Signaling Technology (Danvers, MA). Anti-FADD (05-486, RRID:AB_11212178) was purchased from Merck Millipore (Billerica, MA). Anti-ASC (AL177) (AG-25B-0006, RRID:AB_2490440), anti-NLRP3 (Cryo-2) (AG-20B-0014, RRID:AB_2490202), and anti–caspase-1 (Casper-1) (AG-20B-0042, RRID:AB_2490248) were obtained from AdipoGen Life Science (San Diego, CA). Anti–pro–IL-1β (AF-401-NA, RRID:AB_416684) was purchased from R&D Systems (Minneapolis, MN). Anti–β-actin (sc-69879, RRID:AB_1119529), anti-IκBα (sc-371, RRID:AB_2235952), anti–IL-18 (sc-6179, RRID:AB_2123799), anti–cathepsin-B (sc-365558, RRID:AB_10842446), and anti–caspase-1 (sc-514, RRID:AB_2068895) were purchased from Santa Cruz Biotechnology (Dallas, TX). Anti-HSP90 (610419, RRID:AB_397799) and anti-RIPK1 (610459, RRID:AB_3978320) were obtained from BD Biosciences (Franklin Lakes, NJ). Anti-GSDMD (ab209845, RRID:AB_2783550), anti–caspase-8 (ab138485, RRID:NA), and anti–cathepsin-B (ab214428, RRID:AB_2848144) were purchased from Abcam (Cambridge, UK). Anti–caspase-11 (17D9) (NB120-10454, RRID:AB_788441) was purchased from Novus Biologicals (Centennial, CO).

siGENOME mouse Casp8 siRNA SMARTPool (D-043044), mouse Becn1 siRNA SMARTPool (D-055895), and mouse Atg5 siRNA SMARTPool (M-064838) were obtained from Horizon Discovery Ltd. (Cambridge, UK). Cathepsin-B siRNA (sc-29933) was purchased from Santa Cruz Biotechnology (Dallas, TX). The target sequences for mouse caspase-8 were as follows: 5′-AAUGUAAGCUGGAAGAUGA-3′, 5′-GAACUGCGUUUCCUACCGA-3′, 5′-GAAGUGAGCGAGUUGGAAU-3′, and 5′-AGAGUUGUCUUUAUGCUAU-3′. The siRNA sequences for Atg5 were as follows: 5′-CCAAUUGGUUUACUAUUUG-3′, 5′-CGAAUUCCAACUUGCUUUA-3′, 5′-UUAGUGAGAUAUGGUUUGA-3′, and 5′-GCAUAAAAGUCAAGUGAUC-3′. The siRNA sequences for Becn-1 were as follows: 5′-GGAAGAGGGCUAACUCAGGA-3′, 5′-GGAGUGGAAUGAAAUCAAU-3′, 5′-GGGAGUAUAGUGAGUUUAA-3′, and 5′-GUACCGACUUGUUCCCUAU-3′.

Cell culture

Bone marrow cells were collected from tibias and femurs of age- and sex-matched 8- to 12-week-old mice described in the "Mice" section and cultured in either complete Dulbecco's Modified Eagle's Medium (DMEM) [supplemented with 10% fetal calf serum, 10 mM glutamine, penicillin (100 U/ml), streptomycin (100 μg/ml), and 50 μM 2-mercaptoethanol] with 20% L929 conditioned medium for 6 days to generate BMDMs or complete RPMI (same supplements as for complete DMEM) containing GM-CSF (15 ng/ml) for 8 days to generate BMDCs.

Adenosine triphosphate (ATP) cell viability assays were conducted using the CellTiter-Glo Luminescent Cell Viability Assay Kit (G7570, Promega, Fitchburg, WI). Luminescence was quantitated using the Victor3 1420 Multilabel Counter (PerkinElmer, Shelton, CT). Cell death was also determined by PI staining (*33*) and quantitated under fluorescence microscopy or by using a flow cytometer. Alternatively, lactate dehydrogenase (LDH) release was used to determine the extent of cell death using Cytotoxicity LDH Assay Kit-WST (CK12, Dojindo Molecular Technologies Inc.).

Western blot

For immunoblotting, the culture supernatants were isolated and precipitated by cold acetone (−20°C), and then cells were lysed using whole-cell extract buffer [25 mM Hepes (pH 7.9), 300 mM NaCl, 1.5 mM $MgCl_2$, 0.2 mM EDTA, 0.5 mM dithiothreitol, and 0.1% Triton X-100] on ice for 30 min. Supernatants were separated by centrifugation at 13,200 rpm for 10 min at 4°C. The protein concentrations were determined by Bio-Rad protein assay (#500-00006). Samples were denatured and analyzed by SDS–polyacrylamide gel electrophoresis (SDS-PAGE) in running buffer (0.025 M tris, 0.192 M glycine, and 0.1% SDS). The gel was transferred to polyvinylidene difluoride membrane (Millipore) in transfer buffer (25 mM tris, 192 mM glycine, and 20% methanol) at 400 mA for 100 min at 4°C. Membranes were blocked with SuperBlock T20 (Sigma-Aldrich) to detect anti-phosphate antibody or blocking buffer [5% nonfat milk and 0.1% Tween 20 in a TBST buffer of 50 mM tris-HCl (pH 7.4) and 150 mM NaCl] at room temperature for 30 min, before being incubated overnight at 4°C with specific primary antibodies at indicated dilutions. The membranes were washed three times with wash buffer (0.1% Tween 20 in TBST buffer) at room temperature for 10 min before incubating them with horseradish peroxidase–conjugated secondary antibodies in blocking buffer at room temperature for 1 hour. After washing, the membranes were developed with ECL Western blot detection reagents (Advansta, K-12045-D50), and signals were detected by x-ray film (Fujifilm).

IETD-induced septic shock

Age- and sex-matched 8- to 12-week-old male and female $Fadd^{+/-}Ripk3^{-/-}$ and $Fadd^{-/-}Ripk3^{-/-}$ mice were used. The matched $Fadd^{+/-}Ripk3^{-/-}$ and $Fadd^{-/-}Ripk3^{-/-}$ mice were mostly littermates. Mice were intraperitoneally injected with z-IETD-fmk (5 μg/g) in a total volume of 200 μl endotoxin-free phosphate-buffered saline (PBS). Three hours after injection, mouse blood serum was collected and IL-6 levels were determined using an ELISA kit. Peritoneal lavage was then conducted by rinsing the peritoneum with 0.5 ml of PBS. Cells from peritoneal lavages were stained with PI, and cytokine levels were determined using ELISA kits. For septic shock, the survival of mice was monitored for 30 hours after IETD administration. Age- and sex-matched 8- to 10-week-old $Fadd^{+/-}Ripk3^{-/-}$ and $Fadd^{-/-}Ripk3^{-/-}$ mice carrying $Nlrp3^{-/-}$, $Casp1/11^{-/-}$, $Gsdmd^{-/-}$, or $Becn1^{f/f}LysM^{Cre}$ were further used for septic shock study. Each set of experiment was designed to contain a minimum of five pairs of mice, but a lower number of mice were used (fig. S11, D and F) due to difficulty to obtain sufficient specific triple knockout mice. Also, because of the limited number of the triple knockout mice generated, no experimental randomization was applied. Reagent administration (IETD) and result recording (death monitor) were conducted by different persons, but blinding was not strictly implemented as the readout (mouse death) was clear-cut.

ASC cross-linking

BMDCs were treated with R848 + IETD for 8 hours. Cells were washed with ice-cold PBS and then incubated in buffer A [20 mM Hepes (pH 7.2), 10 mM KCl, 1.5 mM $MgCl_2$, 320 mM sucrose, 1 mM EDTA, and 1 mM EGTA]. Cell lysates were centrifuged to remove cell debris, and the supernatant was then added to a double volume of buffer A before being filtered through 5-μm mesh. Filtered samples were added to a double volume of CHAPS buffer [20 mM Hepes (pH 7.5), 5 mM $MgCl_2$, 0.5 mM EGTA, 0.1 mM phenylmethylsulfonyl fluoride, and 0.1% CHAPS] and then centrifuged at 5000*g* for 8 min. The pellets were resuspended in CHAPS buffer and cross-linked by means of dextran sulfate sodium (4 mM) at room temperature for 30 min. Samples were then boiled before being resolved by SDS-PAGE.

Microscopy

For time-lapse fluorescence microscopy, BMDMs were seeded in 96-well plates. Cells were stimulated with LPS (0.1 μg/ml) and IETD (10 μM) for 1 hour before adding PI (0.2 μg/ml). Images were then acquired using an MD ImageXpress Micro XL microscope over the course of another 15 hours at intervals of 30 min. For DAPGreen staining, BMDMs were stained with DAPGreen (0.2 μM) for 30 min and then stimulated with LPS (0.1 μg/ml) and IETD (10 μM) in the absence or presence of 3-MA (1 mM) for 16 hours. Cell nuclei were stained with Hoechst 33342 Ready Flow reagent. Images were captured using an Olympus IX71 microscope. Average DAPGreen fluorescence intensity in a cell defined by Hoechst staining was quantified by ImageJ. The fold change in fluorescence intensity induced by IETD was compared to that by LPS alone.

IEC culture

Mouse IECs were cultured using IntestiCult Organoid Growth Medium (06005, StemCell Technologies, Vancouver, Canada) following the manufacturer's protocol. In brief, intestine was isolated from age- and sex-matched $Fadd^{+/-}Ripk3^{-/-}$ or $Fadd^{-/-}Ripk3^{-/-}$ mice, washed, and cut open longitudinally. The washed intestinal sheet was cut into 2-mm pieces and then washed 20 times. The tissue pieces were resuspended in Gentle Cell Dissociation Reagent (07174, StemCell) and incubated for 15 min at room temperature. The released intestinal crypts were isolated; aliquoted into 500, 1500, and 3000 crypts per fraction; and pelleted by centrifugation. IntestiCult Organoid Growth Medium was then added to the pellets, followed by Matrigel Matrix (356231, Corning), and each resuspended pellet was placed onto six wells of a 24-well plate. The intestinal crypts were analyzed for their response to LPS + IETD treatment after culturing for 7 to 10 days. LDH release was quantified 24 hours after LPS + IETD treatment.

Statistics

In vitro data were collected randomly but not blind. No samples or animals were excluded from this study. Two or three technical replicates were used for the in vitro experiment, and three independent experiments were conducted. Data met the assumptions of applied statistical tests (i.e., normal distributions). Statistical analyses were conducted in Prism 5 (GraphPad). Results were evaluated by two-way analysis of variance (ANOVA) followed by Sidak's or Tukey's multiple comparisons test, as described in the respective figure legends. A log-rank (Mantel-Cox) test was used to compare mouse survival. Data are presented as means + SD. *P* values of <0.05 were considered significant, as indicated in the figure legends.

SUPPLEMENTARY MATERIALS

Supplementary material for this article is available at https://science.org/doi/10.1126/sciadv.abn9912

View/request a protocol for this paper from *Bio-protocol*.

REFERENCES AND NOTES

1. M. Muzio, A. M. Chinnaiyan, F. C. Kischkel, K. O'Rourke, A. Shevchenko, J. Ni, C. Scaffidi, J. D. Bretz, M. Zhang, R. Gentz, M. Mann, P. H. Krammer, M. E. Peter, V. M. Dixit, FLICE,

a novel FADD-homologous ICE/CED-3-like protease, is recruited to the CD95 (Fas/APO-1) death-inducing signaling complex. *Cell* **85**, 817–827 (1996).
2. M. P. Boldin, T. M. Goncharov, Y. V. Goltsev, D. Wallach, Involvement of MACH, a novel MORT1/FADD-interacting protease, in Fas/APO-1- and TNF receptor-induced cell death. *Cell* **85**, 803–815 (1996).
3. S. Nagata, Apoptosis and clearance of apoptotic cells. *Annu. Rev. Immunol.* **36**, 489–517 (2018).
4. A. Oberst, C. P. Dillon, R. Weinlich, L. L. McCormick, P. Fitzgerald, C. Pop, R. Hakem, G. S. Salvesen, D. R. Green, Catalytic activity of the caspase-8-FLIP(L) complex inhibits RIPK3-dependent necrosis. *Nature* **471**, 363–367 (2011).
5. W. J. Kaiser, J. W. Upton, A. B. Long, D. Livingston-Rosanoff, L. P. Daley-Bauer, R. Hakem, T. Caspary, E. S. Mocarski, RIP3 mediates the embryonic lethality of caspase-8-deficient mice. *Nature* **471**, 368–372 (2011).
6. H. Zhang, X. Zhou, T. McQuade, J. Li, F. K. Chan, J. Zhang, Functional complementation between FADD and RIP1 in embryos and lymphocytes. *Nature* **471**, 373–376 (2011).
7. K. Newton, K. E. Wickliffe, A. Maltzman, D. L. Dugger, R. Reja, Y. Zhang, M. Roose-Girma, Z. Modrusan, M. S. Sagolla, J. D. Webster, V. M. Dixit, Activity of caspase-8 determines plasticity between cell death pathways. *Nature* **575**, 679–682 (2019).
8. M. Fritsch, S. D. Gunther, R. Schwarzer, M. C. Albert, F. Schorn, J. P. Werthenbach, L. M. Schiffmann, N. Stair, H. Stocks, J. M. Seeger, M. Lamkanfi, M. Kronke, M. Pasparakis, H. Kashkar, Caspase-8 is the molecular switch for apoptosis, necroptosis and pyroptosis. *Nature* **575**, 683–687 (2019).
9. P. Broz, V. M. Dixit, Inflammasomes: Mechanism of assembly, regulation and signalling. *Nat. Rev. Immunol.* **16**, 407–420 (2016).
10. K. V. Swanson, M. Deng, J. P. Ting, The NLRP3 inflammasome: Molecular activation and regulation to therapeutics. *Nat. Rev. Immunol.* **19**, 477–489 (2019).
11. N. Kayagaki, I. B. Stowe, B. L. Lee, K. O'Rourke, K. Anderson, S. Warming, T. Cuellar, B. Haley, M. Roose-Girma, Q. T. Phung, P. S. Liu, J. R. Lill, H. Li, J. Wu, S. Kummerfeld, J. Zhang, W. P. Lee, S. J. Snipas, G. S. Salvesen, L. X. Morris, L. Fitzgerald, Y. Zhang, E. M. Bertram, C. C. Goodnow, V. M. Dixit, Caspase-11 cleaves gasdermin D for non-canonical inflammasome signalling. *Nature* **526**, 666–671 (2015).
12. J. Shi, Y. Zhao, K. Wang, X. Shi, Y. Wang, H. Huang, Y. Zhuang, T. Cai, F. Wang, F. Shao, Cleavage of GSDMD by inflammatory caspases determines pyroptotic cell death. *Nature* **526**, 660–665 (2015).
13. X. Liu, Z. Zhang, J. Ruan, Y. Pan, V. G. Magupalli, H. Wu, J. Lieberman, Inflammasome-activated gasdermin D causes pyroptosis by forming membrane pores. *Nature* **535**, 153–158 (2016).
14. J. Maelfait, E. Vercammen, S. Janssens, P. Schotte, M. Haegman, S. Magez, R. Beyaert, Stimulation of Toll-like receptor 3 and 4 induces interleukin-1beta maturation by caspase-8. *J. Exp. Med.* **205**, 1967–1973 (2008).
15. S. I. Gringhuis, T. M. Kaptein, B. A. Wevers, B. Theelen, M. van der Vlist, T. Boekhout, T. B. Geijtenbeek, Dectin-1 is an extracellular pathogen sensor for the induction and processing of IL-1β via a noncanonical caspase-8 inflammasome. *Nat. Immunol.* **13**, 246–254 (2012).
16. J. E. Vince, W. W. Wong, I. Gentle, K. E. Lawlor, R. Allam, L. O'Reilly, K. Mason, O. Gross, S. Ma, G. Guarda, H. Anderton, R. Castillo, G. Häcker, J. Silke, J. Tschopp, Inhibitor of apoptosis proteins limit RIP3 kinase-dependent interleukin-1 activation. *Immunity* **36**, 215–227 (2012).
17. S. Kang, T. Fernandes-Alnemri, C. Rogers, L. Mayes, Y. Wang, C. Dillon, L. Roback, W. Kaiser, A. Oberst, J. Sagara, K. A. Fitzgerald, D. R. Green, J. Zhang, E. S. Mocarski, E. S. Alnemri, Caspase-8 scaffolding function and MLKL regulate NLRP3 inflammasome activation downstream of TLR3. *Nat. Commun.* **6**, 7515 (2015).
18. P. Gurung, P. K. Anand, R. K. Malireddi, L. Vande Walle, N. Van Opdenbosch, C. P. Dillon, R. Weinlich, D. R. Green, M. Lamkanfi, T. D. Kanneganti, FADD and caspase-8 mediate priming and activation of the canonical and noncanonical Nlrp3 inflammasomes. *J. Immunol.* **192**, 1835–1846 (2014).
19. X. Zhang, C. Fan, H. Zhang, Q. Zhao, Y. Liu, C. Xu, Q. Xie, X. Wu, X. Yu, J. Zhang, H. Zhang, MLKL and FADD are critical for suppressing progressive lymphoproliferative disease and activating the NLRP3 inflammasome. *Cell Rep.* **16**, 3247–3259 (2016).
20. B. Tummers, L. Mari, C. S. Guy, B. L. Heckmann, D. A. Rodriguez, S. Ruhl, J. Moretti, J. C. Crawford, P. Fitzgerald, T. D. Kanneganti, L. J. Janke, S. Pelletier, J. M. Blander, D. R. Green, Caspase-8-dependent inflammatory responses are controlled by its adaptor, FADD, and necroptosis. *Immunity* **52**, 994–1006.e8 (2020).
21. R. Allam, K. E. Lawlor, E. C. Yu, A. L. Mildenhall, D. M. Moujalled, R. S. Lewis, F. Ke, K. D. Mason, M. J. White, K. J. Stacey, A. Strasser, L. A. O'Reilly, W. Alexander, B. T. Kile, D. L. Vaux, J. E. Vince, Mitochondrial apoptosis is dispensable for NLRP3 inflammasome activation but non-apoptotic caspase-8 is required for inflammasome priming. *EMBO Rep.* **15**, 982–990 (2014).
22. R. Schwarzer, H. Jiao, L. Wachsmuth, A. Tresch, M. Pasparakis, FADD and caspase-8 regulate gut homeostasis and inflammation by controlling MLKL- and GSDMD-mediated death of intestinal epithelial cells. *Immunity* **52**, 978–993.e6 (2020).
23. T. B. Kang, S. H. Yang, B. Toth, A. Kovalenko, D. Wallach, Caspase-8 blocks kinase RIPK3-mediated activation of the NLRP3 inflammasome. *Immunity* **38**, 27–40 (2013).
24. M. C. Maiuri, E. Zalckvar, A. Kimchi, G. Kroemer, Self-eating and self-killing: Crosstalk between autophagy and apoptosis. *Nat. Rev. Mol. Cell Biol.* **8**, 741–752 (2007).
25. J. Doherty, E. H. Baehrecke, Life, death and autophagy. *Nat. Cell Biol.* **20**, 1110–1117 (2018).
26. L. Yu, A. Alva, H. Su, P. Dutt, E. Freundt, S. Welsh, E. H. Baehrecke, M. J. Lenardo, Regulation of an ATG7-beclin 1 program of autophagic cell death by caspase-8. *Science* **304**, 1500–1502 (2004).
27. J. O. Pyo, M. H. Jang, Y. K. Kwon, H. J. Lee, J. I. Jun, H. N. Woo, D. H. Cho, B. Choi, H. Lee, J. H. Kim, N. Mizushima, Y. Oshumi, Y. K. Jung, Essential roles of Atg5 and FADD in autophagic cell death: Dissection of autophagic cell death into vacuole formation and cell death. *J. Biol. Chem.* **280**, 20722–20729 (2005).
28. B. D. Bell, S. Leverrier, B. M. Weist, R. H. Newton, A. F. Arechiga, K. A. Luhrs, N. S. Morrissette, C. M. Walsh, FADD and caspase-8 control the outcome of autophagic signaling in proliferating T cells. *Proc. Natl. Acad. Sci. U.S.A.* **105**, 16677–16682 (2008).
29. M. M. Young, Y. Takahashi, O. Khan, S. Park, T. Hori, J. Yun, A. K. Sharma, S. Amin, C. D. Hu, J. Zhang, M. Kester, H. G. Wang, Autophagosomal membrane serves as platform for intracellular death-inducing signaling complex (iDISC)-mediated caspase-8 activation and apoptosis. *J. Biol. Chem.* **287**, 12455–12468 (2012).
30. J. Zhang, D. Cado, A. Chen, N. H. Kabra, A. Winoto, Fas-mediated apoptosis and activation-induced T-cell proliferation are defective in mice lacking FADD/Mort1. *Nature* **392**, 296–300 (1998).
31. C. L. Evavold, J. Ruan, Y. Tan, S. Xia, H. Wu, J. C. Kagan, The pore-forming protein gasdermin D regulates interleukin-1 secretion from living macrophages. *Immunity* **48**, 35–44.e6 (2018).
32. J. J. Hu, X. Liu, S. Xia, Z. Zhang, Y. Zhang, J. Zhao, J. Ruan, X. Luo, X. Lou, Y. Bai, J. Wang, L. R. Hollingsworth, V. G. Magupalli, L. Zhao, H. R. Luo, J. Kim, J. Lieberman, H. Wu, FDA-approved disulfiram inhibits pyroptosis by blocking gasdermin D pore formation. *Nat. Immunol.* **21**, 736–745 (2020).
33. N. Lalaoui, S. E. Boyden, H. Oda, G. M. Wood, D. L. Stone, D. Chau, L. Liu, M. Stoffels, T. Kratina, K. E. Lawlor, K. J. M. Zaal, P. M. Hoffmann, N. Etemadi, K. Shield-Artin, C. Biben, W. L. Tsai, M. D. Blake, H. S. Kuehn, D. Yang, H. Anderton, N. Silke, L. Wachsmuth, L. Zheng, N. S. Moura, D. B. Beck, G. Gutierrez-Cruz, A. K. Ombrello, G. P. Pinto-Patarroyo, A. J. Kueh, M. J. Herold, C. Hall, H. Wang, J. J. Chae, N. I. Dmitrieva, M. McKenzie, A. Light, B. K. Barham, A. Jones, T. M. Romeo, Q. Zhou, I. Aksentijevich, J. C. Mullikin, A. J. Gross, A. K. Shum, E. D. Hawkins, S. L. Masters, M. J. Lenardo, M. Boehm, S. D. Rosenzweig, M. Pasparakis, A. K. Voss, M. Gadina, D. L. Kastner, J. Silke, Mutations that prevent caspase cleavage of RIPK1 cause autoinflammatory disease. *Nature* **577**, 103–108 (2020).
34. V. G. Magupalli, R. Negro, Y. Tian, A. V. Hauenstein, G. Di Caprio, W. Skillern, Q. Deng, P. Orning, H. B. Alam, Z. Maliga, H. Sharif, J. J. Hu, C. L. Evavold, J. C. Kagan, F. I. Schmidt, K. A. Fitzgerald, T. Kirchhausen, Y. Li, H. Wu, HDAC6 mediates an aggresome-like mechanism for NLRP3 and pyrin inflammasome activation. *Science* **369**, eaas8995 (2020).
35. D. Chauvier, S. Ankri, C. Charriaut-Marlangue, R. Casimir, E. Jacotot, Broad-spectrum caspase inhibitors: From myth to reality? *Cell Death Differ.* **14**, 387–391 (2007).
36. L. Sun, Z. Wu, Y. Hayashi, C. Peters, M. Tsuda, K. Inoue, H. Nakanishi, Microglial cathepsin B contributes to the initiation of peripheral inflammation-induced chronic pain. *J. Neurosci.* **32**, 11330–11342 (2012).
37. P. Schotte, W. Van Criekinge, M. Van de Craen, G. Van Loo, M. Desmedt, J. Grooten, M. Cornelissen, L. De Ridder, J. Vandekerckhove, W. Fiers, P. Vandenabeele, R. Beyaert, Cathepsin B-mediated activation of the proinflammatory caspase-11. *Biochem. Biophys. Res. Commun.* **251**, 379–387 (1998).
38. M. Bruchard, G. Mignot, V. Derangere, F. Chalmin, A. Chevriaux, F. Vegran, W. Boireau, B. Simon, B. Ryffel, J. L. Connat, J. Kanellopoulos, F. Martin, C. Rebe, L. Apetoh, F. Ghiringhelli, Chemotherapy-triggered cathepsin B release in myeloid-derived suppressor cells activates the Nlrp3 inflammasome and promotes tumor growth. *Nat. Med.* **19**, 57–64 (2013).
39. K. Newton, K. E. Wickliffe, D. L. Dugger, A. Maltzman, M. Roose-Girma, M. Dohse, L. Komuves, J. D. Webster, V. M. Dixit, Cleavage of RIPK1 by caspase-8 is crucial for limiting apoptosis and necroptosis. *Nature* **574**, 428–431 (2019).
40. Y. Lin, A. Devin, Y. Rodriguez, Z. G. Liu, Cleavage of the death domain kinase RIP by caspase-8 prompts TNF-induced apoptosis. *Genes Dev.* **13**, 2514–2526 (1999).
41. A. Rajput, A. Kovalenko, K. Bogdanov, S. H. Yang, T. B. Kang, J. C. Kim, J. Du, D. Wallach, RIG-I RNA helicase activation of IRF3 transcription factor is negatively regulated by caspase-8-mediated cleavage of the RIP1 protein. *Immunity* **34**, 340–351 (2011).
42. P. Tao, J. Sun, Z. Wu, S. Wang, J. Wang, W. Li, H. Pan, R. Bai, J. Zhang, Y. Wang, P. Y. Lee, W. Ying, Q. Zhou, J. Hou, W. Wang, B. Sun, M. Yang, D. Liu, R. Fang, H. Han, Z. Yang, X. Huang, H. Li, N. Deuitch, Y. Zhang, D. Dissanayake, K. Haude, K. McWalter, C. Roadhouse, J. J. MacKenzie, R. M. Laxer, I. Aksentijevich, X. Yu, X. Wang, J. Yuan, Q. Zhou, A dominant autoinflammatory disease caused by non-cleavable variants of RIPK1. *Nature* **577**, 109–114 (2020).
43. K. Nakahira, J. A. Haspel, V. A. Rathinam, S. J. Lee, T. Dolinay, H. C. Lam, J. A. Englert, M. Rabinovitch, M. Cernadas, H. P. Kim, K. A. Fitzgerald, S. W. Ryter, A. M. Choi, Autophagy

proteins regulate innate immune responses by inhibiting the release of mitochondrial DNA mediated by the NALP3 inflammasome. *Nat. Immunol.* **12**, 222–230 (2011).
44. Z. Zhong, A. Umemura, E. Sanchez-Lopez, S. Liang, S. Shalapour, J. Wong, F. He, D. Boassa, G. Perkins, S. R. Ali, M. D. McGeough, M. H. Ellisman, E. Seki, A. B. Gustafsson, H. M. Hoffman, M. T. Diaz-Meco, J. Moscat, M. Karin, NF-κB restricts inflammasome activation via elimination of damaged mitochondria. *Cell* **164**, 896–910 (2016).
45. H. Li, P. Wang, Q. Sun, W. X. Ding, X. M. Yin, R. W. Sobol, D. B. Stolz, J. Yu, L. Zhang, Following cytochrome c release, autophagy is inhibited during chemotherapy-induced apoptosis by caspase 8-mediated cleavage of Beclin 1. *Cancer Res.* **71**, 3625–3634 (2011).
46. S. Huang, K. Okamoto, C. Yu, F. A. Sinicrope, p62/sequestosome-1 up-regulation promotes ABT-263-induced caspase-8 aggregation/activation on the autophagosome. *J. Biol. Chem.* **288**, 33654–33666 (2013).
47. X. Zhang, J. P. Dowling, J. Zhang, RIPK1 can mediate apoptosis in addition to necroptosis during embryonic development. *Cell Death Dis.* **10**, 245 (2019).
48. C. Watts, Capture and processing of exogenous antigens for presentation on MHC molecules. *Annu. Rev. Immunol.* **15**, 821–850 (1997).
49. I. Rauch, K. A. Deets, D. X. Ji, J. von Moltke, J. L. Tenthorey, A. Y. Lee, N. H. Philip, J. S. Ayres, I. E. Brodsky, K. Gronert, R. E. Vance, NAIP-NLRC4 inflammasomes coordinate intestinal epithelial cell expulsion with eicosanoid and IL-18 release via activation of caspase-1 and -8. *Immunity* **46**, 649–659 (2017).

Acknowledgments: We thank C.-Y. Tsai and staff of the Transgenic Core Facility of Academia Sinica for generating the RIPK3 knockout mouse line, Y. Lin and staff of the FACS Core of the Institute of Molecular Biology Academia Sinica (IMB) for cell sorting, S.-P. Lee and staff of the Confocal Core of IMB for confocal microscopy, and J. O'Brien for editing the manuscript. **Funding:** This work was funded by Ministry of Science and Technology, Taiwan, R.O.C., grant MOST109-2326-B-001-008 (M.-Z.L.) and Institute of Molecular Biology, Academia Sinica (M.-Z.L.). **Ethics statement:** The experiments in this manuscript did not involve human participants, human data, or human tissue. All animal experiments were conducted with approval from the Institutional Animal Care and Utilization Committee, Academia Sinica. **Author contributions:** Conceptualization: M.-Z.L. Methodology: Y.-H.W., S.-L.H., and J.Z. Investigation: Y.-H.W., S.-T.M., I.-T.C., and F.-Y.H. Visualization: Y.-H.W., S.-T.M., and F.-Y.H. Supervision: M.-Z.L. Writing—original draft: Y.-H.W. and M.-Z.L. Writing—review and editing: J.Z. and M.-Z.L. **Competing interests:** The authors declare that they have no competing interests. **Data and materials availability:** All data needed to evaluate the conclusions in the paper are present in the paper and/or the Supplementary Materials.

Submitted 6 January 2022
Accepted 27 September 2022
Published 11 November 2022
10.1126/sciadv.abn9912

ScienceAdvances

Caspase-8 inactivation drives autophagy-dependent inflammasome activation in myeloid cells

Yung-Hsuan WuShu-Ting MoI-Ting ChenFu-Yi HsiehShie-Liang HsiehJinake ZhangMing-Zong Lai

Sci. Adv., 8 (45), eabn9912. • DOI: 10.1126/sciadv.abn9912

Science Advances (ISSN) is published by the American Association for the Advancement of Science. 1200 New York Avenue NW, Washington, DC 20005. The title *Science Advances* is a registered trademark of AAAS.